MULTISCALE MODEL. SIMUL.
Vol. 16, No. 2, pp. 954–990

SCATTERING BY A PERIODIC ARRAY OF SUBWAVELENGTH SLITS II: SURFACE BOUND STATES, TOTAL TRANSMISSION, AND FIELD ENHANCEMENT IN HOMOGENIZATION REGIMES*

JUNSHAN LIN† AND HAI ZHANG‡

Abstract. This is the second part in a series of two papers that are concerned with the quantitative analysis of the electromagnetic field enhancement and anomalous diffraction by a periodic array of subwavelength slits in a perfect conducting slab. In this part, we explore the scattering problem in the homogenization regimes, where the period of the structure is much smaller than the incident wavelength. In particular, two homogenization regimes are investigated: in the first regime, the width of the slits is comparable to the period, while in the second regime, the width of the slits is much smaller than the period. By presenting rigorous asymptotic analysis, we demonstrate that a surface plasmonic effect mimicking that of plasmonic metals occurs in the first regime. In addition, for incident plane waves, we discover and justify a novel phenomenon of total transmission which occurs either at certain frequencies for all incident angles or at a special incident angle but for all frequencies. For the second regime, the nonresonant field enhancement is investigated. It is shown that the fast transition of the magnetic field in the slits induces strong electric field enhancement. Moreover, the enhancement becomes stronger when the coupling between the slits is weaker.

Key words. electromagnetic field enhancement, total transmission, subwavelength structure, surface bound states, surface plasmon, homogenization

AMS subject classifications. 35C20, 35Q60, 35P30

DOI. 10.1137/17M1133786

1. Introduction.

This is the second part in a series of two papers that are concerned with the electromagnetic scattering and field enhancement for a perfect conducting slab patterned with a periodic array of subwavelength slits. In the first part [24], we investigated the field enhancement in the diffraction regime, where the period of the metallic structure is of the same order as the incident wavelength. In this paper, we explore the scattering problem in the homogenization regime, where the size of the period is much smaller than the incident wavelength. We shall consider two homogenization regimes. In the first regime, the width of the pattered slits has the same order as the period of the slab (see Figure 2, top), while in the second regime, the width is much smaller than the period (see Figure 2, bottom). The studies are motivated by recent growing interest in extraordinary optical transmission and strongly enhanced electromagnetic fields in subwavelength apertures or holes, which could lead to potentially significant applications in biological and chemical sensing, near-field spectroscopy, etc. [11, 13, 14, 15, 19, 28]. We remark that a similar homogenization regime has been investigated for periodically arranged subwavelength resonators such as plasmonic particles and bubbles in [4, 5], where the mechanism of metasurface is explained. The reader is also referred to [23] for scattering and field

*Received by the editors June 9, 2017; accepted for publication (in revised form) December 20, 2017; published electronically May 17, 2018.
http://www.siam.org/journals/mms/16-2/M113378.html
Funding: The first author was partially supported by NSF grants DMS-1417676 and DMS-1719851. The second author was partially supported by Hong Kong RGC grant ECS 26301016 and UGC grant SBI17SC12 from HKUST.
†Department of Mathematics and Statistics, Auburn University, Auburn, AL 36849 (jzl0097@auburn.edu).
‡Department of Mathematics, HKUST, Clear Water Bay, Kowloon, Hong Kong (haizhang@ust.hk).

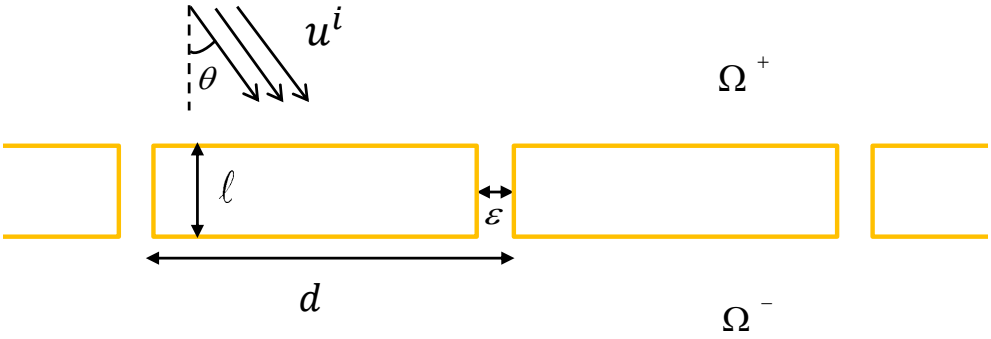

FIG. 1. *Setup of the scattering problem. The slits S_ε are arranged periodically with the size of the period d, and each slit has a rectangular shape of length ℓ and width ε, respectively. The domains above and below the perfect conductor slab are denoted as Ω^+ and Ω^-, respectively, and the domain exterior to the perfect conductor is denoted as Ω_ε, which consists of S_ε, Ω^+, and Ω^-.*

enhancement for a single narrow slit and [8, 10] for a closely related problem of scattering by subwavelength cavities.

We now present the setup of the scattering problem. Figure 1 depicts the geometry of the cross section for the metallic structure under consideration. The slab occupies the domain $\{(x_1, x_2) \mid 0 < x_2 < \ell\}$ on the x_1x_2 plane, where ℓ is the thickness of the metallic slab. The slits, which are invariant along the x_3 direction, occupy the region $S_\varepsilon = \bigcup_{n=-\infty}^{\infty}(S_\varepsilon^{(0)} + nd)$, where d is the size of the period, and $S_\varepsilon^{(0)} := \{(x_1, x_2) \mid 0 < x_1 < \varepsilon, 0 < x_2 < \ell\}$. We denote the semi-infinite domains above and below the slab by Ω^+ and Ω^-, respectively, and the domain exterior to the perfect conductor by Ω_ε, i.e., $\Omega_\varepsilon = \Omega^+ \cup \Omega^- \cup S_\varepsilon$. We also denote by ν the unit outward normal pointing to the exterior domain Ω^+ or Ω^-.

The width of slit ε is assumed to be much smaller than the thickness of the slab ℓ. For clarity of exposition, we shall set $\ell = 1$ in all technical derivations. The general case for $\ell \neq 1$ follows by a normalization process and a scaling argument. Furthermore, we assume that the size of the period d is much smaller than the wavelength λ such that the problem under consideration is in the homogenization regime. The following two homogenization regimes are investigated here:

(H1) The scale of geometrical parameters are given by $\ell = 1$, $\varepsilon \sim d \ll 1$, and the incident wavelength $\lambda \sim O(1)$ or $\lambda \gg 1$. That is, $\varepsilon \sim d \ll \lambda$. A schematic plot of the geometry is shown in Figure 2 (top).

(H2) The scale of geometrical parameters are given by $\ell = 1$, $\varepsilon \ll 1$, $d \sim 1$ or $1 \ll d \ll \lambda$, and $\lambda \gg 1$. That is, $\varepsilon \ll d \ll \lambda$. A schematic plot of the geometry is shown in Figure 2 (bottom).

Assume that a polarized time-harmonic electromagnetic wave impinges upon the perfect conductor from above. We consider the transverse magnetic (TM) case where the incident magnetic field is perpendicular to the x_1x_2 plane, and its x_3 component is given by the scalar function $u^i = e^{i(\kappa x_1 - \zeta(x_2-1))}$. Here $\kappa = k\sin\theta$, $\zeta = k\cos\theta$, k is the wavenumber, and θ is the incident angle. Throughout the paper, we assume that $|\theta| < \theta_0 < \frac{\pi}{2}$ for some θ_0 to exclude the case of grazing incidence angle. The total field u_ε, which consists of the incident wave u^i and the scattered field u_ε^s, satisfies the Helmholtz equation

$$\Delta u_\varepsilon + k^2 u_\varepsilon = 0 \qquad \text{in } \Omega_\varepsilon \tag{1.1}$$

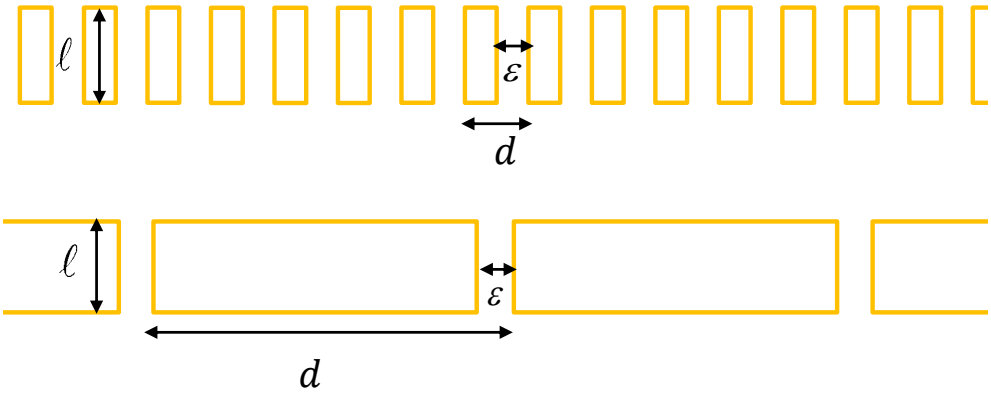

FIG. 2. *Geometry of slits in two homogenization regimes. Top:* $\ell = 1$, $\varepsilon \sim d \ll 1$, *Bottom:* $\ell = 1$. $\varepsilon \ll 1$, $d \sim 1$, *or* $d \gg 1$ *but* $d \ll \lambda$.

and the boundary condition

$$\frac{\partial u_\varepsilon}{\partial \nu} = 0 \quad \text{on } \partial\Omega_\varepsilon. \tag{1.2}$$

We look for quasi-periodic solutions such that $u_\varepsilon(x_1, x_2) = e^{i\kappa x_1}\tilde{u}_\varepsilon(x_1, x_2)$, where $\tilde{u}_\varepsilon$ is a periodic function with $\tilde{u}_\varepsilon(x_1 + d, x_2) = \tilde{u}_\varepsilon(x_1, x_2)$, or equivalently,

$$u_\varepsilon(x_1 + d, x_2) = e^{i\kappa d}u_\varepsilon(x_1, x_2). \tag{1.3}$$

Define

$$\kappa_n = \kappa + \frac{2\pi n}{d} \quad \text{and} \quad \zeta_n(k) = \sqrt{k^2 - \kappa_n^2},$$

where the function $f(z) = \sqrt{z}$ is understood as an analytic function defined in the domain $\mathbf{C}\backslash\{-it : t \geq 0\}$ by

$$\sqrt{z} = |z|^{\frac{1}{2}} e^{\frac{1}{2} i \arg z}$$

throughout the paper. Then it can be shown that the outgoing scattered field adopts the following Rayleigh–Bloch expansion in Ω^+ and Ω^-, respectively (cf. [6, 7, 31]):

$$u_\varepsilon^s(x_1, x_2) = \sum_{n=-\infty}^{\infty} u_n^{s,+} e^{i\kappa_n x_1 + i\zeta_n x_2} \quad \text{and} \quad u_\varepsilon^s(x_1, x_2) = \sum_{n=-\infty}^{\infty} u_n^{s,-} e^{i\kappa_n x_1 - i\zeta_n x_2}, \tag{1.4}$$

where $u_n^{s,\pm}$ are constants. The expansion (1.4) is usually referred to as the outgoing radiation condition and is imposed for the scattered field in the two semi-infinite domains. In sum, the mathematical model for the scattering problem is defined in the domain Ω_ε and given by (1.1)–(1.4). Due to the quasi periodicity of the solution, we will restrict κ to the first Brillouin zone $(-\pi/d, \pi/d]$. Such κ is called the reduced wave vector component [7, 31].

In this paper, based upon a combination of layer potential techniques and asymptotic analysis, we present quantitative analysis of field enhancement and anomalous transmission behavior for the scattering problem in the above mentioned two homogenization regimes:

(i) In the homogenization regime (H1), the asymptotic expansions of the dispersion relation and the associated eigenmodes of the structure are derived, which demonstrate the existence of surface plasmonic effect mimicking that of plasmonic metals. More precisely, the dispersion curve, which lies below the light line with $k(\kappa) < |\kappa|$, resembles that of surface plasmon polaritons of metallic slabs made of noble metals, and the eigenmodes, which are surface bound states along the boundaries of the perfect conducting slab, resemble the plasmonic waves of noble metals. Therefore, the specific configuration with $\varepsilon \sim d \ll \lambda$ in this regime extends the frequency band for the surface plasmon, which is originally supported on noble metals in an optical and near-infrared regime, to the lower frequency regime where metals can be viewed as perfect conductors. This is the so-called spoof surface plasmon in the physics literature and has the potential for openning new opportunities to control radiation at surfaces over a wide spectral range [14, 28].
We further derive the asymptotic expansion of the scattered wave field when an incident plane wave impinges on the periodic structure. In such a scenario, $|\kappa| = |k \sin\theta| < k$ and the solution to the scattering problem (1.1)–(1.4) is unique. Interestingly, it is shown that total transmission through the slab structure can be achieved either at certain frequencies for all incident angles or for all frequencies at a specific incident angle. We clarify that such perfect transmission is not due to a plasmonic resonant effect or scattering resonance. Instead, the former is related to as Fabry–Perot resonance associated with the homogenized homogeneous slab, where all reflected waves from the slab boundaries interfere destructively [33], while the latter can be attributed to the Brewster angle effect [2, 3].

(ii) In the homogenization regime (H2), we show that there exists no complex resonance or real eigenvalue, and the scattering problem (1.1)–(1.4) attains a unique solution. We derive the asymptotic expansion of the wave fields and show that although no enhancement is gained for the magnetic field, a strong electric field is induced in the slits and on the slit apertures. Such field enhancement is induced not by resonances but due to the fast transition of the magnetic field in the slits. In addition, we discuss the enhancement with varying period d. We show that as the period d decreases and the coupling between the slits is stronger, the field enhancement becomes weaker.

The rest of the paper is organized as follows. We begin by introducing layer potentials for the scattering problem and presenting the asymptotic expansion for the solution to the scattering problem in section 2 for both homogenization regimes. The quantitative analysis of anomalous transmission and field enhancement behaviors is presented in sections 3 and 4 for the homogenization regimes (H1) and (H2), respectively. The paper is concluded with some remarks about ongoing and future works along this direction in section 5.

2. Boundary integral equations and the solution to the scattering problem.

2.1. Layer potentials and boundary integral formulations. In this section, we collect some preliminaries on the layer potentials and boundary integral formulations for the scattering problem. The reader is referred to the first part of this series [24] for the proof. For a given $\kappa \in (-\pi/d, \pi/d]$, let

$$g^d(x,y) = g^d(x,y;\kappa) = -\frac{i}{2d}\sum_{n=-\infty}^{\infty}\frac{1}{\zeta_n(k)}e^{i\kappa_n(x_1-y_1)+i\zeta_n(k)|x_2-y_2|}, \tag{2.1}$$

where

$$\kappa_n = \kappa + \frac{2\pi n}{d} \quad \text{and} \quad \zeta_n(k) = \begin{cases} \sqrt{k^2 - \kappa_n^2}, & |\kappa_n| < k, \\ i\sqrt{\kappa_n^2 - k^2}, & |\kappa_n| > k. \end{cases}$$

It is clear that $g^d(x, y, \kappa)$ is the quasi-periodic Green function which solves the following equation:

$$\Delta g^d(x, y; \kappa) + k^2 g^d(x, y; \kappa) = e^{i\kappa(x_1 - y_1)} \sum_{n=-\infty}^{\infty} \delta(x_1 - y_1 - nd)\delta(x_2 - y_2), \quad x, y \in \mathbf{R}^2.$$

The exterior Green function $g^e(x, y) = g^e(x, y, \kappa)$ in domain $\Omega^+ \cup \Omega^-$ with the Neumann boundary condition $\frac{\partial g^e(x,y,\kappa)}{\partial \nu_y} = 0$ on $\{y_2 = 1\}$ and $\{y_2 = 0\}$ is then given by $g^e(x, y) = g^d(x, y, \kappa) + g^d(x', y, \kappa)$, where

$$x' = \begin{cases} (x_1, 2 - x_2) & \text{if } x, y \in \Omega^+, \\ (x_1, -x_2) & \text{if } x, y \in \Omega^-. \end{cases}$$

The Green function $g^i_\varepsilon(x, y)$ that solves

$$\Delta g^i_\varepsilon(x, y) + k^2 g^i_\varepsilon(x, y) = \delta(x - y), \quad x, y \in S^{(0)}_\varepsilon,$$

with the Neumann boundary condition may be expressed as

$$g^i_\varepsilon(x, y) = \sum_{m,n=0}^{\infty} c_{mn}\phi_{mn}(x)\phi_{mn}(y),$$

where $c_{mn} = \frac{1}{k^2 - (m\pi/\varepsilon)^2 - (n\pi)^2}$, $\phi_{mn} = \sqrt{\frac{a_{mn}}{\varepsilon}} \cos(\frac{m\pi x_1}{\varepsilon}) \cos(n\pi x_2)$ with the coefficient

$$a_{mn} = \begin{cases} 1 & m = n = 0, \\ 2 & m = 0, n \geq 1, \quad \text{or} \quad n = 0, m \geq 1, \\ 4 & m \geq 1, n \geq 1. \end{cases}$$

To formulate the boundary integral equations, we consider the reference cell $\Omega^{(0)} := \{x \in \mathbf{R}^2 \mid 0 < x_1 < d\}$ as shown in Figure 3. Denote the upper and lowers apertures of the slit $S^{(0)}_\varepsilon$ in $\Omega^{(0)}$ by Γ^+_ε and Γ^-_ε, respectively (see Figure 3).

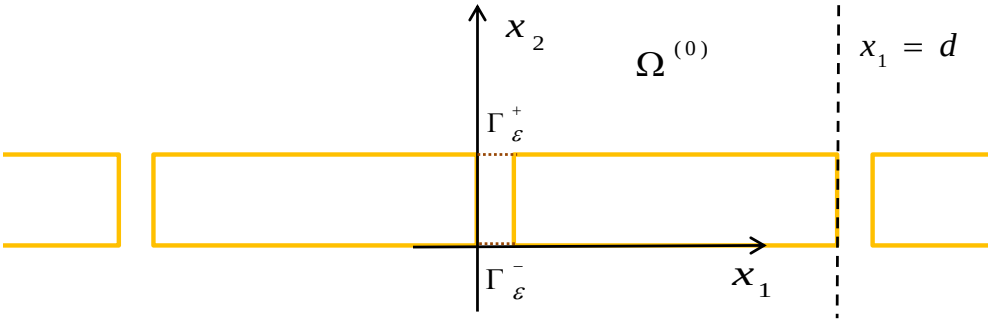

FIG. 3. *Problem geometry in one reference period* $\Omega^{(0)}$.

LEMMA 2.1 (see [24]). *Let $u_\varepsilon(x)$ be the solution of the scattering problem* (1.1)–(1.4)*; then*

$$u_\varepsilon(x) = \int_{\Gamma_\varepsilon^+} g^e(x,y)\frac{\partial u_\varepsilon(y)}{\partial y_2}ds_y + u^i + u^r \quad \text{for } x \in \Omega^{(0)} \cap \Omega^+,$$

$$u_\varepsilon(x) = -\int_{\Gamma_\varepsilon^-} g^e(x,y)\frac{\partial u_\varepsilon(y)}{\partial y_2}ds_y \quad \text{for } x \in \Omega^{(0)} \cap \Omega^-,$$

$$u_\varepsilon(x) = \int_{\Gamma_\varepsilon^-} g_\varepsilon^i(x,y)\frac{\partial u_\varepsilon(y)}{\partial y_2}ds_y - \int_{\Gamma_\varepsilon^+} g_\varepsilon^i(x,y)\frac{\partial u_\varepsilon(y)}{\partial y_2}ds_y \quad \text{for } x \in S_\varepsilon^{(0)}.$$

Here $u^r = e^{i(\kappa x_1 + \zeta(x_2-1))}$ is the reflected field by the ground plane $\{x_2 = 1\}$ without slits.

Based upon Lemma 2.1 and the continuity of the single layer potential, we obtain the following boundary integral equations defined over the slit apertures $\Gamma_\varepsilon^\pm$.

LEMMA 2.2. *The following hold for the solution of the scattering problem* (1.1)–(1.4)*:*

$$u_\varepsilon(x) = \int_{\Gamma_\varepsilon^+} g^e(x,y)\frac{\partial u_\varepsilon(y)}{\partial y_2}ds_y + u^i + u^r \quad \text{for } x \in \Gamma_\varepsilon^+, \tag{2.2}$$

$$u_\varepsilon(x) = -\int_{\Gamma_\varepsilon^-} g^e(x,y)\frac{\partial u_\varepsilon(y)}{\partial y_2}ds_y \quad \text{for } x \in \Gamma_\varepsilon^-, \tag{2.3}$$

$$u_\varepsilon(x) = \int_{\Gamma_\varepsilon^-} g_\varepsilon^i(x,y)\frac{\partial u_\varepsilon(y)}{\partial y_2}ds_y - \int_{\Gamma_\varepsilon^+} g_\varepsilon^i(x,y)\frac{\partial u_\varepsilon(y)}{\partial y_2}ds_y \quad \text{for } x \in \Gamma_\varepsilon^+ \cup \Gamma_\varepsilon^-. \tag{2.4}$$

An application of the above lemma leads to the following system of integral equations:

$$\begin{cases} \displaystyle\int_{\Gamma_\varepsilon^+} g^e(x,y)\frac{\partial u_\varepsilon(y)}{\partial y_2}ds_y + \int_{\Gamma_\varepsilon^+} g_\varepsilon^i(x,y)\frac{\partial u_\varepsilon(y)}{\partial y_2}ds_y \\ \qquad\qquad - \displaystyle\int_{\Gamma_\varepsilon^-} g_\varepsilon^i(x,y)\frac{\partial u_\varepsilon(y)}{\partial y_2}ds_y + u^i + u^r = 0 \quad \text{on } \Gamma_\varepsilon^+, \\ \displaystyle -\int_{\Gamma_\varepsilon^-} g^e(x,y)\frac{\partial u_\varepsilon(y)}{\partial y_2}ds_y + \int_{\Gamma_\varepsilon^+} g_\varepsilon^i(x,y)\frac{\partial u_\varepsilon(y)}{\partial y_2}ds_y \\ \qquad\qquad - \displaystyle\int_{\Gamma_\varepsilon^-} g_\varepsilon^i(x,y)\frac{\partial u_\varepsilon(y)}{\partial y_2}ds_y = 0, \quad \text{on } \Gamma_\varepsilon^-. \end{cases} \tag{2.5}$$

PROPOSITION 2.3. *The scattering problem* (1.1)–(1.4) *is equivalent to the system of boundary integral equations* (2.5).

It is clear that

$$\left.\frac{\partial u_\varepsilon}{\partial \nu}\right|_{\Gamma_\varepsilon^+} = \frac{\partial u_\varepsilon}{\partial y_2}(y_1, 1), \quad \left.\frac{\partial u_\varepsilon}{\partial \nu}\right|_{\Gamma_\varepsilon^-} = -\frac{\partial u_\varepsilon}{\partial y_2}(y_1, 0), \quad (u^i + u^r)|_{\Gamma_\varepsilon^+} = 2e^{i\kappa x_1}.$$

The above functions are defined over the slit apertures with width $\varepsilon \ll 1$. We rescale these functions by introducing $X = x_1/\varepsilon$ and $Y = y_1/\varepsilon$, and we define

$$\varphi_1(Y) := -\frac{\partial u_\varepsilon}{\partial y_2}(\varepsilon Y, 1);$$

$$\varphi_2(Y) := \frac{\partial u_\varepsilon}{\partial y_2}(\varepsilon Y, 0);$$

$$f(X) := (u^i + u^r)(\varepsilon X, 1) = 2e^{i\kappa\varepsilon X};$$

$$
\begin{aligned}
G^e_\varepsilon(X,Y) &= G^e_\varepsilon(X,Y,\kappa) := g^e(\varepsilon X,1;\varepsilon Y,1) = g^e(\varepsilon X,0;\varepsilon Y,0)\\
&= -\frac{i}{d}\sum_{n=-\infty}^{\infty}\frac{1}{\zeta_n(k)}e^{i\kappa_n\varepsilon(X-Y)};\\
G^i_\varepsilon(X,Y) &:= g^i_\varepsilon(\varepsilon X,1;\varepsilon Y,1) = g^i_\varepsilon(\varepsilon X,0;\varepsilon Y,0)\\
&= \sum_{m,n=0}^{\infty}\frac{c_{mn}a_{mn}}{\varepsilon}\cos(m\pi X)\cos(m\pi Y);\\
\tilde{G}^i_\varepsilon(X,Y) &:= g^i_\varepsilon(\varepsilon X,1;\varepsilon Y,0) = g^i_\varepsilon(\varepsilon X,0;\varepsilon Y,1)\\
&= \sum_{m,n=0}^{\infty}\frac{(-1)^n c_{mn}a_{mn}}{\varepsilon}\cos(m\pi X)\cos(m\pi Y).
\end{aligned}
$$

We also define three boundary integral operators:

$$(T^e\varphi)(X) = \int_0^1 G^e_\varepsilon(X,Y)\varphi(Y)dY \quad X\in(0,1); \tag{2.6}$$

$$(T^i\varphi)(X) = \int_0^1 G^i_\varepsilon(X,Y)\varphi(Y)dY \quad X\in(0,1); \tag{2.7}$$

$$(\tilde{T}^i\varphi)(X) = \int_0^1 \tilde{G}^i_\varepsilon(X,Y)\varphi(Y)dY \quad X\in(0,1). \tag{2.8}$$

By a change of variable $x_1 = \varepsilon X$ and $y_1 = \varepsilon Y$ in (2.5), the following proposition follows.

PROPOSITION 2.4. *The system of equations* (2.5) *is equivalent to the following one:*

$$\begin{bmatrix} T^e+T^i & \tilde{T}^i \\ \tilde{T}^i & T^e+T^i \end{bmatrix}\begin{bmatrix}\varphi_1\\ \varphi_2\end{bmatrix} = \begin{bmatrix} f/\varepsilon \\ 0\end{bmatrix}. \tag{2.9}$$

2.2. Asymptotic expansion of the boundary integral operators. We introduce several function spaces that are used throughout the paper; see also [24]. Let $H^s(\mathbf{R})$ be the standard fractional Sobolev space for $s\in\mathbf{R}$. For a bounded open interval I, define the Hilbert spaces

$$H^s(I) := \{u = U|_I \;\big|\; U\in H^s(\mathbf{R})\}$$

and

$$\tilde{H}^s(I) := \{u = U|_I \;\big|\; U\in H^s(\mathbf{R}) \text{ and } \operatorname{supp} U\subset \bar{I}\}.$$

Then $\tilde{H}^s(I)$ is the dual of $H^s(I)$. For simplicity of notation, we denote $V_1 = \tilde{H}^{-\frac{1}{2}}(0,1)$ and $V_2 = H^{\frac{1}{2}}(0,1)$. The duality between V_1 and V_2 will be denoted by $\langle u,v\rangle$ for any $u\in V_1$, $v\in V_2$.

Let us define the operator $P: V_1\to V_2$ by

$$P\varphi(X) = \langle\varphi,1\rangle 1, \tag{2.10}$$

where 1 is a function defined on the interval $(0,1)$ and is equal to one therein. Then $1\in V_2$ and the above definition is valid.

To obtain the solution of the scattering problem, we begin with the asymptotic expansion of the integral operators T^e, T^i, and $\tilde{T}^i$. First, the kernels $G^i_\varepsilon(X,Y)$ and $\tilde{G}^i_\varepsilon(X,Y)$ attain the following asymptotic expansions.

LEMMA 2.5. *Let*

$$\beta^i(k,\varepsilon) = \frac{\cot k}{k\varepsilon} + \frac{2\ln 2}{\pi}, \quad \tilde{\beta}(k,\varepsilon) = \frac{1}{(k\sin k)\varepsilon}, \tag{2.11}$$

$$\rho^i(X,Y) = \frac{1}{\pi}\left[\ln\left(\left|\sin\left(\frac{\pi(X+Y)}{2}\right)\right|\right) + \ln\left(\left|\sin\left(\frac{\pi(X-Y)}{2}\right)\right|\right)\right]. \tag{2.12}$$

If $k\varepsilon \ll 1$, *then*

$$G^i_\varepsilon(X,Y) = \beta^i(k,\varepsilon) + \rho^i(X,Y) + r^i_\varepsilon(X,Y),$$
$$\tilde{G}^i_\varepsilon(X,Y) = \tilde{\beta}(k,\varepsilon) + \tilde{r}_\varepsilon(X,Y).$$

Here $r^i_\varepsilon(X,Y)$ *and* $\tilde{r}_\varepsilon(X,Y)$ *are bounded functions with*

$$r^i_\varepsilon \sim O((k\varepsilon)^2) \quad \textit{and} \quad \tilde{r}_\varepsilon \sim O(e^{-1/\varepsilon})$$

for all $X, Y \in (0,1)$.

The proof of the lemma can be found in [23, 24].

LEMMA 2.6. *Assume that* $\kappa \in (-\pi/d, \pi/d]$ *and* $\kappa \sim O(1)$ *satisfying* $|\kappa/\sqrt{k^2-\kappa^2}| \le C$, *where* C *is a positive constant. Then the kernel* $G^e_\varepsilon(X,Y)$ *attains the following asymptotic expansion in both homogenization regimes* (H1) *and* (H2)*:*

$$G^e_\varepsilon(X,Y) = \beta^e(k,\kappa,d,\varepsilon) + \rho^e(X,Y;k,\kappa) + r^e_\varepsilon(X,Y;k,\kappa), \tag{2.13}$$

where $\beta^e(k,\kappa,d,\varepsilon)$ *is independent of* X *and* Y, $\rho^e(X,Y;k,\kappa)$ *is a function independent of* ε, *and* $r^e_\varepsilon(X,Y)$ *is a bounded function with* $r^e_\varepsilon \sim O(r(\varepsilon))$. *In addition,*

$$r(\varepsilon) \to 0 \quad \textit{as} \quad \varepsilon \to 0.$$

(1) *In the homogenization regime* (H1),

$$\beta^e(k,\kappa,d,\varepsilon) = \frac{1}{\pi}\ln 2 - \frac{i\eta}{\sqrt{k^2-\kappa^2}\,\varepsilon}, \tag{2.14}$$

$$\rho^e(X,Y;k,\kappa) = \frac{1}{\pi}\ln|\sin(\pi\eta(X-Y))| + \frac{\kappa\eta}{\sqrt{k^2-\kappa^2}}(X-Y), \tag{2.15}$$

where $\eta = \varepsilon/d$. *In addition,* $r(\varepsilon) = \varepsilon$ *if* $\kappa \neq 0$ *and* $r(\varepsilon) = \varepsilon^2$ *if* $\kappa = 0$.

(2) *In the homogenization regime* (H2),

$$\beta^e(k,\kappa,d,\varepsilon) = \frac{1}{\pi}\left(\ln\varepsilon + \ln 2 + \ln\frac{\pi}{d}\right) + \left(\frac{1}{2\pi}\sum_{n\neq 0}\frac{1}{|n|} - \frac{i}{d}\sum_{n=-\infty}^{\infty}\frac{1}{\zeta_n(k)}\right) \tag{2.16}$$

and

$$\rho^e(X,Y;k,\kappa) = \frac{1}{\pi}\ln(|X-Y|). \tag{2.17}$$

In addition, $r(\varepsilon) = \varepsilon$ *if* $\kappa \neq 0$ *and* $r(\varepsilon) = \varepsilon^2\ln\varepsilon$ *if* $\kappa = 0$.

Remark 2.1. In the above, the expression

$$\frac{1}{2\pi}\sum_{n\neq 0}\frac{1}{|n|} - \frac{i}{d}\sum_{n=-\infty}^{\infty}\frac{1}{\zeta_n(k)}$$

is understood as

$$\sum_{n\neq 0}\left(\frac{1}{2\pi}\frac{1}{|n|}-\frac{i}{d}\frac{1}{\zeta_n(k)}\right)-\frac{i}{d}\frac{1}{\zeta_0(k)},$$

where the series is convergent. Hence, the scalar function $\beta_e(k,\kappa,d,\varepsilon)$ is well defined.

Proof. We derive the asymptotic expansion for the kernel G_ε^e when $\kappa=0$. In the homogenization regime (H1), we have $kd\ll 1$. Therefore,

$$\begin{aligned}
\sum_{n\neq 0}\frac{1}{\zeta_n(k)}e^{i\kappa_n\varepsilon(X-Y)} &= -\frac{id}{2\pi}\sum_{n\neq 0}\frac{1}{|n|\sqrt{1-(kd/2\pi n)^2}}e^{i\frac{2\pi n}{d}\varepsilon(X-Y)}\\
&= -\frac{id}{2\pi}\sum_{n\neq 0}\frac{1}{|n|}\left(1+\sum_{m=1}^{\infty}\frac{1\cdot 3\cdots(2m-1)}{2^m m!}\left(\frac{kd}{2\pi n}\right)^{2m}\right)e^{i\frac{2\pi n}{d}\varepsilon(X-Y)}\\
&= -\frac{id}{2\pi}\sum_{n\neq 0}\frac{1}{|n|}e^{i\frac{2\pi n}{d}\varepsilon(X-Y)}\\
&\quad -\frac{id}{2\pi}\sum_{m=1}^{\infty}\frac{1\cdot 3\cdots(2m-1)}{2^m m!}\sum_{n\neq 0}\left(\frac{kd}{2\pi n}\right)^{2m}\frac{1}{|n|}e^{i\frac{2\pi n}{d}\varepsilon(X-Y)}\\
&= \frac{id}{2\pi}\ln\left(4\sin^2(\pi\eta(X-Y))\right)+O(k^2\varepsilon^3),
\end{aligned}$$

where we have used the formula (cf. [18])

$$\sum_{n\neq 0}\frac{1}{|n|}e^{i\frac{2\pi n}{d}\varepsilon(X-Y)}=\ln\left(4\sin^2\frac{\pi\varepsilon(X-Y)}{d}\right).$$

Therefore,

$$\begin{aligned}
G_\varepsilon^e(X,Y) &= -\frac{i}{d}\sum_{n=-\infty}^{\infty}\frac{1}{\zeta_n(k)}e^{i\kappa_n\varepsilon(X-Y)}\\
&= -\frac{i}{\zeta_0(k)d}+\frac{1}{2\pi}\ln\left(4\sin^2(\pi\eta(X-Y))\right)+O(k^2\varepsilon^2).
\end{aligned}$$

The desired asymptotic expansion follows.

In the homogenization regime (H2), we have $k\ll 1$ and $\varepsilon\ll 1$. Applying the Taylor expansion yields

$$\begin{aligned}
\sum_{n\neq 0}\frac{1}{\zeta_n(k)}e^{i\kappa_n\varepsilon(X-Y)} &= -\frac{id}{2\pi}\sum_{n\neq 0}\frac{1}{|n|\sqrt{1-(kd/2\pi n)^2}}e^{i\frac{2\pi n}{d}\varepsilon(X-Y)}\\
&= -\frac{id}{2\pi}\sum_{n\neq 0}\frac{1}{|n|}\left(1+\sum_{m=1}^{\infty}\frac{1\cdot 3\cdots(2m-1)}{2^m m!}\left(\frac{kd}{2\pi n}\right)^{2m}\right)e^{i\frac{2\pi n}{d}\varepsilon(X-Y)}.
\end{aligned}$$

By the formula

$$-\sum_{n\neq 0}\frac{1}{|n|}e^{i\frac{2\pi n}{d}\varepsilon(X-Y)}=\ln\left(4\sin^2\frac{\pi\varepsilon(X-Y)}{d}\right),$$

and noting that for $m\geq 1$ (cf. [20]),

$$\sum_{n\neq 0}\frac{1}{|n|^{2m+1}}e^{i\frac{2\pi n}{d}\varepsilon(X-Y)}=\sum_{n\neq 0}\frac{1}{|n|^{2m+1}}+O(\varepsilon^{2m}(X-Y)^{2m})\ln(\varepsilon(X-Y)),$$

we obtain

$$\begin{aligned}
&\sum_{n\neq 0}\frac{1}{\zeta_n(k)}e^{i\kappa_n\varepsilon(X-Y)}\\
&\quad=\frac{id}{2\pi}\ln\left(4\sin^2\frac{\pi\varepsilon(X-Y)}{d}\right)\\
&\qquad-\frac{id}{2\pi}\sum_{m=1}^{\infty}\frac{1\cdot 3\cdots(2m-1)}{2^m m!}\sum_{n\neq 0}\left(\frac{kd}{2\pi}\right)^{2m}\frac{1}{|n|^{2m+1}}+O(\varepsilon^2\ln\varepsilon).\\
&\quad=\frac{id}{2\pi}\ln\left(4\sin^2\frac{\pi\varepsilon(X-Y)}{d}\right)-\frac{id}{2\pi}\left(\sum_{n\neq 0}\frac{1}{|n|\sqrt{1-(kd/2\pi n)^2}}-\frac{1}{|n|}\right)+O(\varepsilon^2\ln\varepsilon)\\
&\quad=\frac{id}{2\pi}\ln\left(4\sin^2\frac{\pi\varepsilon(X-Y)}{d}\right)+\frac{id}{2\pi}\sum_{n\neq 0}\frac{1}{|n|}+\sum_{n\neq 0}\frac{1}{\zeta_n(k)}+O(\varepsilon^2\ln\varepsilon).
\end{aligned}$$

The desired asymptotic expansion follows by noting that $\varepsilon \ll d$ and using the expansion

$$G^e_\varepsilon(X,Y)=-\frac{i}{d}\sum_{n=-\infty}^{\infty}\frac{1}{\zeta_n(k)}e^{i\kappa_n\varepsilon(X-Y)}=-\frac{i}{d}\left(\frac{1}{\zeta_0(k)}+\sum_{n\neq 0}\frac{1}{\zeta_n(k)}e^{i\kappa_n\varepsilon(X-Y)}\right).$$

Following similar procedures as above, the asymptotic expansion of the kernel for $\kappa\neq 0$ in both homogenization regimes can be obtained, by noting that

$$-\frac{i}{d}\frac{1}{\zeta_0(k)}e^{i\kappa\varepsilon(X-Y)}=-\frac{i}{\sqrt{k^2-\kappa^2}d}\left(1+i\kappa\varepsilon(X-Y)+\kappa^2\cdot O(\varepsilon^2)\right). \qquad \square$$

Let

$$\beta=\beta^i+\beta^e, \tag{2.18}$$

where β^i is defined in (2.11), and β^e is defined by (2.14) and (2.16) for two homogenization regimes, respectively. Set

$$\begin{aligned}
\rho(X,Y;k,\kappa)&=\rho^i(X,Y)+\rho^e(X,Y;k,\kappa),\\
\rho_\infty(X,Y;k,\kappa)&=r^i_\varepsilon(X,Y)+r^e_\varepsilon(X,Y;k,\kappa),\\
\tilde\rho_\infty(X,Y)&=\tilde r_\varepsilon(X,Y),
\end{aligned}$$

where ρ^i is given by (2.12), ρ^e is given by (2.15) and (2.17) for two homogenization regimes, respectively, and r^i_ε, $\tilde r_\varepsilon$, and r^e_ε are the high-order terms as specified in Lemmas 2.5 and 2.6. We define three integral operators K, K_∞, $\tilde K_\infty$ by letting

$$(K\varphi)(X)=\int_0^1\rho(X,Y;k,\kappa)\varphi(Y)dY,\quad X\in(0,1); \tag{2.19}$$

$$(K_\infty\varphi)(X)=\int_0^1\rho_\infty(X,Y;k,\kappa)\varphi(Y)dY,\quad X\in(0,1); \tag{2.20}$$

$$(\tilde K_\infty\ \varphi)(X)=\int_0^1\tilde\rho_\infty(X,Y)\varphi(Y)dY,\quad X\in(0,1). \tag{2.21}$$

Remark 2.2. Note that in the above, the function β and the kernels of the integral operators ρ, ρ_∞, and $\tilde{\rho}_\infty$ take different forms in the homogenization regimes (H1) and (H2). Here and henceforth, we adopt the same notation for the sake of presenting a unified asymptotic framework for the scattering problem (see section 2.3). However, their values should be clear from the context.

LEMMA 2.7. *Let the assumption in Lemma* 2.6 *hold; then in both homogenization regimes, the operator K is bounded from V_1 to V_2 with a bounded inverse. Moreover,*

$$\alpha(k,\kappa) := \langle K^{-1}1, 1\rangle \text{ is a real number and } \alpha(k,\kappa) \neq 0.$$

Remark 2.3. α takes different values in the two homogenization regimes. It depends on k, κ in the former homogenization regime, and is independent of k and κ in the latter. For ease of notation, we will simply denote it as α in the rest of the paper.

Proof. The proof for the homogenization regime (H1) is postponed to the appendix. For the homogenization regime (H2), recall the kernel of the K takes the form

$$\rho(X,Y;k,\kappa) = \frac{1}{\pi}\ln|X-Y| + \frac{1}{\pi}\left[\ln\left(\left|\sin\left(\frac{\pi(X+Y)}{2}\right)\right|\right) + \ln\left(\left|\sin\left(\frac{\pi(X-Y)}{2}\right)\right|\right)\right],$$

which is independent of k, κ. The proof can be found in Theorem 4.1 and Lemma 4.2 of [8]. ∎

LEMMA 2.8. *Let the assumption in Lemma* 2.6 *hold; then the following holds for* (H1) *and* (H2)*:*

(1) *The operator $T^e + T^i$ admits the following decomposition:*

$$T^e + T^i = \beta P + K + K_\infty.$$

Moreover, K_∞ is bounded from V_1 to V_2 with the operator norm $\|K_\infty\| \lesssim r(\varepsilon)$ uniformly for bounded k.

(2) *The operator $\tilde{T}^i$ admits the following decomposition:*

$$\tilde{T}^i = \tilde{\beta} P + \tilde{K}_\infty,$$

Moreover, $\tilde{K}_\infty$ is bounded from V_1 to V_2 with the operator norm $\|K_\infty\| \lesssim e^{-1/\varepsilon}$ uniformly for bounded k.

Proof. From the definition of T^e and T^i, the kernel of $T^e + T^i$ is $G^e_\varepsilon(X,Y) + G^i_\varepsilon(X,Y)$. By the asymptotic expansions of the kernels in Lemmas 2.5 and 2.6, it is clear that

$$\begin{aligned} G^e_\varepsilon(X,Y) + G^i_\varepsilon(X,Y) &= \beta^e + \beta^i + \rho^e(X,Y;k,\kappa) + \rho^i(X,Y) + r^e_\varepsilon(X,Y;k,\kappa) + r^i_\varepsilon(X,Y) \\ &= \beta + \rho(X,Y;k,\kappa) + \rho_\infty(X,Y). \end{aligned}$$

The assertion (1) then follows from (2.19) and (2.20). The proof of (2) follows by using the decomposition

$$\tilde{G}^i_\varepsilon(X,Y) = \tilde{\beta}(k,\varepsilon) + \tilde{r}_\varepsilon(X,Y) = \tilde{\beta}(k,\varepsilon) + \tilde{\rho}_\infty(X,Y). \qquad ∎$$

2.3. Asymptotic expansion of the solution to the scattering problem. For both homogenization regimes, we define

$$\mathbb{P} = \begin{bmatrix} \beta P & \tilde{\beta} P \\ \tilde{\beta} P & \beta P \end{bmatrix}, \quad \mathbb{K}_\infty = \begin{bmatrix} K_\infty & \tilde{K}_\infty \\ \tilde{K}_\infty & K_\infty \end{bmatrix}, \quad \mathbf{f} = \begin{bmatrix} f/\varepsilon \\ 0 \end{bmatrix}, \quad \text{and} \quad \mathbb{L} = K\mathbb{I} + \mathbb{K}_\infty.$$

Then from the decomposition of the operators in Lemma 2.8, we may rewrite the system of the integral equations (2.9) as

$$(\mathbb{P} + \mathbb{L})\boldsymbol{\varphi} = \mathbf{f}. \tag{2.22}$$

Next, we derive the asymptotic expansion of the solution $\boldsymbol{\varphi}$. By Lemma 2.7, it is also easy to see that $\mathbb{L}$ is invertible for sufficiently small ε. Applying the Neumann series yields

$$\mathbb{L}^{-1} = (K\mathbb{I} + \mathbb{K}_\infty)^{-1} = \left(\sum_{j=0}^{\infty} (-1)^j \left(K^{-1}\mathbb{K}_\infty \right)^j \right) K^{-1} = K^{-1}\mathbb{I} + O\left(r(\varepsilon)\right).$$

Therefore, the following lemma follows immediately.

LEMMA 2.9. *Let* $\mathbf{e}_1 = [1,0]^T$ *and* $\mathbf{e}_2 = [0,1]^T$. *Then*

$$\mathbb{L}^{-1}\mathbf{e}_1 = K^{-1}1 \cdot \mathbf{e}_1 + O(r(\varepsilon)), \quad \mathbb{L}^{-1}\mathbf{e}_2 = K^{-1}1 \cdot \mathbf{e}_2 + O(r(\varepsilon)), \tag{2.23}$$

and

$$\langle \mathbb{L}^{-1}\mathbf{e}_1, \mathbf{e}_1 \rangle = \alpha + O(r(\varepsilon)), \quad \langle \mathbb{L}^{-1}\mathbf{e}_1, \mathbf{e}_2 \rangle = O(r(\varepsilon)). \tag{2.24}$$

Here α *is defined in Lemma* 2.7.

LEMMA 2.10. *Let* $\mathbf{e}_1 = [1,0]^T$ *and* $\mathbf{e}_2 = [0,1]^T$. *Then*

$$\langle \mathbb{L}^{-1}\mathbf{e}_1, \mathbf{e}_1 \rangle = \langle \mathbb{L}^{-1}\mathbf{e}_2, \mathbf{e}_2 \rangle, \quad \langle \mathbb{L}^{-1}\mathbf{e}_1, \mathbf{e}_2 \rangle = \langle \mathbb{L}^{-1}\mathbf{e}_2, \mathbf{e}_1 \rangle.$$

Proof. Let $\mathbb{L}^{-1}\mathbf{e}_1 = (a,b)^T$. Then $\mathbb{L}(a,b)^T = \mathbf{e}_1$. More precisely,

$$\begin{aligned} Ka + K_\infty a + \tilde{K}_\infty b &= 1, \\ Kb + \tilde{K}_\infty a + K_\infty b &= 0. \end{aligned}$$

It follows that $\mathbb{L}(b,a)^T = \mathbf{e}_2$, or equivalently,

$$\mathbb{L}^{-1}\mathbf{e}_2 = (b,a)^T,$$

hence the two identities hold. ∎

By applying $\mathbb{L}^{-1}$ on both sides of (2.22), we see that

$$\mathbb{L}^{-1}\,\mathbb{P}\,\boldsymbol{\varphi} + \boldsymbol{\varphi} = \mathbb{L}^{-1}\mathbf{f}. \tag{2.25}$$

Note that

$$\mathbb{P}\,\boldsymbol{\varphi} = \beta\langle \boldsymbol{\varphi}, \mathbf{e}_1 \rangle \mathbf{e}_1 + \beta\langle \boldsymbol{\varphi}, \mathbf{e}_2 \rangle \mathbf{e}_2 + \tilde{\beta}\langle \boldsymbol{\varphi}, \mathbf{e}_2 \rangle \mathbf{e}_1 + \tilde{\beta}\langle \boldsymbol{\varphi}, \mathbf{e}_1 \rangle \mathbf{e}_2;$$

the above operator equation can be written as

$$\beta\langle \boldsymbol{\varphi}, \mathbf{e}_1 \rangle \mathbb{L}^{-1}\mathbf{e}_1 + \beta\langle \boldsymbol{\varphi}, \mathbf{e}_2 \rangle \mathbb{L}^{-1}\mathbf{e}_2 + \tilde{\beta}\langle \boldsymbol{\varphi}, \mathbf{e}_2 \rangle \mathbb{L}^{-1}\mathbf{e}_1 + \tilde{\beta}\langle \boldsymbol{\varphi}, \mathbf{e}_1 \rangle \mathbb{L}^{-1}\mathbf{e}_2 + \boldsymbol{\varphi} = \mathbb{L}^{-1}\mathbf{f}. \tag{2.26}$$

By taking the inner product of (2.26) with $\mathbf{e}_1$ and $\mathbf{e}_2$, respectively, it follows that

$$(\mathbb{M}+\mathbb{I})\begin{bmatrix}\langle\boldsymbol{\varphi},\mathbf{e}_1\rangle\\ \langle\boldsymbol{\varphi},\mathbf{e}_2\rangle\end{bmatrix}=\begin{bmatrix}\langle\mathbb{L}^{-1}\mathbf{f},\mathbf{e}_1\rangle\\ \langle\mathbb{L}^{-1}\mathbf{f},\mathbf{e}_2\rangle\end{bmatrix}, \tag{2.27}$$

where the matrix $\mathbb{M}$ is defined as

$$\mathbb{M}:=\beta\begin{bmatrix}\langle\mathbb{L}^{-1}\mathbf{e}_1,\mathbf{e}_1\rangle & \langle\mathbb{L}^{-1}\mathbf{e}_2,\mathbf{e}_1\rangle\\ \langle\mathbb{L}^{-1}\mathbf{e}_1,\mathbf{e}_2\rangle & \langle\mathbb{L}^{-1}\mathbf{e}_2,\mathbf{e}_2\rangle\end{bmatrix}+\tilde{\beta}\begin{bmatrix}\langle\mathbb{L}^{-1}\mathbf{e}_2,\mathbf{e}_1\rangle & \langle\mathbb{L}^{-1}\mathbf{e}_1,\mathbf{e}_1\rangle\\ \langle\mathbb{L}^{-1}\mathbf{e}_2,\mathbf{e}_2\rangle & \langle\mathbb{L}^{-1}\mathbf{e}_1,\mathbf{e}_2\rangle\end{bmatrix}. \tag{2.28}$$

From Lemma 2.10, it is observed that

$$\mathbb{M}=\left(\beta+\tilde{\beta}\begin{bmatrix}0&1\\1&0\end{bmatrix}\right)\begin{bmatrix}\langle\mathbb{L}^{-1}\mathbf{e}_1,\mathbf{e}_1\rangle & \langle\mathbb{L}^{-1}\mathbf{e}_1,\mathbf{e}_2\rangle\\ \langle\mathbb{L}^{-1}\mathbf{e}_1,\mathbf{e}_2\rangle & \langle\mathbb{L}^{-1}\mathbf{e}_1,\mathbf{e}_1\rangle\end{bmatrix}.$$

A straightforward calculation shows that the eigenvalues of $\mathbb{M}+\mathbb{I}$ are

$$\lambda_1(k;\kappa,d,\varepsilon)=1+(\beta+\tilde{\beta})\left(\langle\mathbb{L}^{-1}\mathbf{e}_1,\mathbf{e}_1\rangle+\langle\mathbb{L}^{-1}\mathbf{e}_1,\mathbf{e}_2\rangle\right), \tag{2.29}$$

$$\lambda_2(k;\kappa,d,\varepsilon)=1+(\beta-\tilde{\beta})\left(\langle\mathbb{L}^{-1}\mathbf{e}_1,\mathbf{e}_1\rangle-\langle\mathbb{L}^{-1}\mathbf{e}_1,\mathbf{e}_2\rangle\right), \tag{2.30}$$

and the associated eigenvectors are $[1\quad 1]^T$ and $[1\quad -1]^T$, respectively. For simplicity of notation, let us define

$$p(k;\kappa,d,\varepsilon):=\varepsilon\lambda_1(k;\kappa,d,\varepsilon)\quad\text{and}\quad q(k;\kappa,d,\varepsilon):=\varepsilon\lambda_2(k;\kappa,d,\varepsilon), \tag{2.31}$$

which will be used throughout the rest of the paper.

Solving (2.27) leads to

$$\begin{bmatrix}\langle\boldsymbol{\varphi},\mathbf{e}_1\rangle\\ \langle\boldsymbol{\varphi},\mathbf{e}_2\rangle\end{bmatrix}=(\mathbb{M}+\mathbb{I})^{-1}\begin{bmatrix}\langle\mathbb{L}^{-1}\mathbf{f},\mathbf{e}_1\rangle\\ \langle\mathbb{L}^{-1}\mathbf{f},\mathbf{e}_2\rangle\end{bmatrix}. \tag{2.32}$$

By substituting into (2.25), we obtain the solution to the integral equation system (2.9):

$$\boldsymbol{\varphi}=\mathbb{L}^{-1}\mathbf{f}-\begin{bmatrix}\mathbb{L}^{-1}\mathbf{e}_1 & \mathbb{L}^{-1}\mathbf{e}_2\end{bmatrix}\begin{bmatrix}\beta&\tilde{\beta}\\ \tilde{\beta}&\beta\end{bmatrix}(\mathbb{M}+\mathbb{I})^{-1}\begin{bmatrix}\langle\mathbb{L}^{-1}\mathbf{f},\mathbf{e}_1\rangle\\ \langle\mathbb{L}^{-1}\mathbf{f},\mathbf{e}_2\rangle\end{bmatrix}. \tag{2.33}$$

LEMMA 2.11. *Assume that $k\in\mathbf{R}^+$ is not a singular frequency. Let $\kappa=k\sin\theta$, where θ is the incident angle. Then the following asymptotic expansion holds for the solution $\boldsymbol{\varphi}$ to* (2.9) *in $V_1\times V_1$ in both homogenization regimes:*

$$\boldsymbol{\varphi}=K^{-1}1\cdot\left[\kappa\cdot O(1)\cdot\mathbf{e}_1+\frac{\alpha}{p}(\mathbf{e}_1+\mathbf{e}_2)+\frac{\alpha}{q}(\mathbf{e}_1-\mathbf{e}_2)\right]+\left(\frac{\alpha}{p}+\frac{\alpha}{q}\right)\cdot O(r(\varepsilon))+O(r(\varepsilon)).$$

Moreover,

$$\begin{bmatrix}\langle\boldsymbol{\varphi},\mathbf{e}_1\rangle\\ \langle\boldsymbol{\varphi},\mathbf{e}_2\rangle\end{bmatrix}=[\alpha+O(r(\varepsilon))]\left(\frac{1}{p}\begin{bmatrix}1\\1\end{bmatrix}+\frac{1}{q}\begin{bmatrix}1\\-1\end{bmatrix}\right). \tag{2.34}$$

Here α is defined in Lemma 2.7*, and p and q are defined by* (2.31).

Proof. For given k and κ, we see that $\zeta:=\sqrt{k^2-\kappa^2}=k\cos\theta$. Thus $\kappa/\zeta=\tan\theta$ is bounded and the assumption in Lemmas 2.6 and 2.8 holds. Note that the matrix

$\mathbb{M}+\mathbb{I}$ has two eigenvalues λ_1 and λ_2 given by (2.29) and (2.30), which are associated with the eigenvectors $[1 \quad 1]^T$ and $[1 \quad -1]^T$, respectively. Therefore

$$(\mathbb{M}+\mathbb{I})^{-1} = \frac{1}{2\lambda_1}\begin{bmatrix} 1 & 1 \\ 1 & 1 \end{bmatrix} + \frac{1}{2\lambda_2}\begin{bmatrix} 1 & -1 \\ -1 & 1 \end{bmatrix}.$$

Substituting into (2.32) and (2.33) yields

$$\begin{bmatrix} \langle \boldsymbol{\varphi}, \mathbf{e}_1 \rangle \\ \langle \boldsymbol{\varphi}, \mathbf{e}_2 \rangle \end{bmatrix} = \frac{1}{2\lambda_1}\langle \mathbb{L}^{-1}\mathbf{f}, \mathbf{e}_1 + \mathbf{e}_2 \rangle \begin{bmatrix} 1 \\ 1 \end{bmatrix} + \frac{1}{2\lambda_2(k,\varepsilon)}\langle \mathbb{L}^{-1}\mathbf{f}, \mathbf{e}_1 - \mathbf{e}_2 \rangle \begin{bmatrix} 1 \\ -1 \end{bmatrix}$$

and

$$\begin{aligned} \boldsymbol{\varphi} = \mathbb{L}^{-1}\mathbf{f} &+ \frac{1-\lambda_1/\langle \mathbb{L}^{-1}\mathbf{e}_1, \mathbf{e}_1+\mathbf{e}_2\rangle}{2\lambda_1}\langle \mathbb{L}^{-1}\mathbf{f}, \mathbf{e}_1+\mathbf{e}_2\rangle \cdot (\mathbb{L}^{-1}\mathbf{e}_1 + \mathbb{L}^{-1}\mathbf{e}_2) \\ &+ \frac{1-\lambda_2(k,\varepsilon)/\langle \mathbb{L}^{-1}\mathbf{e}_1, \mathbf{e}_1+\mathbf{e}_2\rangle}{2\lambda_2(k,\varepsilon)}\langle \mathbb{L}^{-1}\mathbf{f}, \mathbf{e}_1-\mathbf{e}_2\rangle \cdot (\mathbb{L}^{-1}\mathbf{e}_1 - \mathbb{L}^{-1}\mathbf{e}_2). \end{aligned} \tag{2.35}$$

From the Taylor expansion of $\mathbf{f}$ and the asymptotic expansion of the operator $\mathbb{L}^{-1}$ in Lemma 2.9, we can obtain the desired asymptotic expansions for $\boldsymbol{\varphi}$, $\langle \boldsymbol{\varphi}, \mathbf{e}_1 \rangle$, $\langle \boldsymbol{\varphi}, \mathbf{e}_2 \rangle$. This derivation is similar to Lemma 3.5 of the first part of this series [24], and we omit here. ∎

2.4. An overview of diffraction anomaly and field enhancement. From Lemma 2.11, we see that the solution $\boldsymbol{\varphi}$ to the system of integral equations (2.9) depends on the two functions p and q. In the rest of the paper, we investigate their properties in both homogenization regimes and explore the anomalous behaviors and field enhancement for the scattering problem.

In the homogenization regime (H1), we will shown that for each κ, there exist roots for $p(k;\kappa,d,\varepsilon) = 0$ and $q(k;\kappa,d,\varepsilon) = 0$ such that the homogeneous scattering problem attains nontrivial solutions. These roots give the dispersion relation of the surface modes of the underling periodic structure. Very interestingly, the first branch of the dispersion curve $k(\kappa)$ and the corresponding surface modes resemble those of surface plasmon polaritons of metallic slabs made of noble metals. This is the so-called spoof surface plasmon [14, 28]. It extends the frequency band for the surface plasmon, which is originally supported on a flat noble metal in an optical and near-infrared regime, to the terahertz or lower frequency regime where metals are nearly perfect conductors. We will derive the asymptotic expansions for the dispersion curve and the associated eigenmodes in section 3. A discussion of the surface plasmonic effect will also be presented. It is also demonstrated that total transmission can be achieved. More precisely, for an incident plane wave, there exist certain frequencies such that no wave is reflected, and all electromagnetic energy passes through the slab in the limit of $\varepsilon \to 0$. Such a phenomenon also occurs for all frequencies at a specific incident angle. These results will also be reported in section 3.

In the homogenization regime (H2), it will be shown that no roots exist for $p(k;\kappa,d,\varepsilon) = 0$ and $q(k;\kappa,d,\varepsilon) = 0$, and the periodic structure supports no surface modes or resonance modes. However, significant electric field enhancement still occurs in and near the slits. These will be investigated in section 4.

3. Homogenization regime (H1): Surface bound states and total transmission. In the homogenization regime (H1), the scale of parameters is given by $\varepsilon \sim d \ll 1$ (Figure 2, top). We adopt the notation $\eta := \varepsilon/d$ for the ratio between

the slit width and the size of the period. We derive the asymptotic expansions of the dispersion relation and the corresponding eigenmodes of the periodic structure in sections 3.1 and 3.2. The effective medium theory for the periodic structure as $\varepsilon \to 0$ is presented in section 3.3, which recovers the leading order of the dispersion relation given in section 3.1. A brief discussion on the surface plasmon effect of the perfect conducting slab with slits and that of the plasmonic metallic slab is given in section 3.4.

The other phenomenon induced by the given periodic structure is the total transmission through the small slits when an incident plane wave impinges on the slab. This occurs either at certain frequencies for all incident angles or for all frequencies at a specific incident angle. More precisely, no wave is reflected, and all electromagnetic energy passes through the slab in the limiting case of $\varepsilon \to 0$. We derive the field pattern above and below the slab for the scattering problem in section 3.3 and discuss the total transmission phenomenon in section 3.5.

3.1. Asymptotic expansions of the dispersion relation. To obtain the dispersion relation, we consider the homogeneous scattering problem with incident wave $u^i = 0$. By (2.22), the homogeneous problem is equivalent to the operator equation

$$(\mathbb{P} + \mathbb{L})\boldsymbol{\varphi} = 0.$$

In light of (2.27), this reduces to

$$(\mathbb{M} + \mathbb{I}) \begin{bmatrix} \langle \boldsymbol{\varphi}, \mathbf{e}_1 \rangle \\ \langle \boldsymbol{\varphi}, \mathbf{e}_2 \rangle \end{bmatrix} = 0,$$

where the matrix $\mathbb{M}$ is defined by (2.28). Therefore, the characteristic values of the operator-valued function $\mathbb{P}+\mathbb{L}$, or equivalently the singular frequencies, are the roots of $\lambda_1(k;\kappa,d,\varepsilon)$ and $\lambda_2(k;\kappa,d,\varepsilon)$, the eigenvalues of $\mathbb{M}+\mathbb{I}$. Then one only needs to solve $p(k;\kappa,d,\varepsilon)=0$ and $q(k;\kappa,d,\varepsilon)=0$ to obtain the singular frequencies.

In light of (2.29), and the definition of β in (2.18), and Lemma 2.9, we may explicitly express p as follows:

$$\begin{aligned} p(k;\kappa,d,\varepsilon) &= \varepsilon + \left[\left(\frac{\cot k}{k} + \frac{1}{k\sin k} - \frac{i\eta}{\sqrt{k^2-\kappa^2}}\right) + \frac{3\ln 2}{\pi}\varepsilon\right]\left(\langle \mathbb{L}^{-1}\mathbf{e}_1, \mathbf{e}_1\rangle + \langle \mathbb{L}^{-1}\mathbf{e}_1, \mathbf{e}_2\rangle\right) \\ &= \varepsilon + \left[\left(\frac{\cot k}{k} + \frac{1}{k\sin k} - \frac{i\eta}{\sqrt{k^2-\kappa^2}}\right) + \frac{3\ln 2}{\pi}\varepsilon\right](\alpha + s(\varepsilon)), \end{aligned} \tag{3.1}$$

where $s(\varepsilon) \sim O(r(\varepsilon))$. Similarly,

$$q(k;\kappa,d,\varepsilon) = \varepsilon + \left[\left(\frac{\cot k}{k} - \frac{1}{k\sin k} - \frac{i\eta}{\sqrt{k^2-\kappa^2}}\right) + \frac{3\ln 2}{\pi}\varepsilon\right](\alpha + t(\varepsilon)), \tag{3.2}$$

where $t(\varepsilon) \sim O(r(\varepsilon))$. First, we investigate the roots for the leading-order terms of p and q.

LEMMA 3.1. *For each κ,*

$$c_\pm(k,\kappa) = \frac{\cot k}{k} \pm \frac{1}{k\sin k} - \frac{i\eta}{\sqrt{k^2-\kappa^2}} = 0$$

attains real roots $k^\pm_{m,0}(\kappa)$ $(m = 0, 1, 2, \ldots, M^\pm)$. In addition,

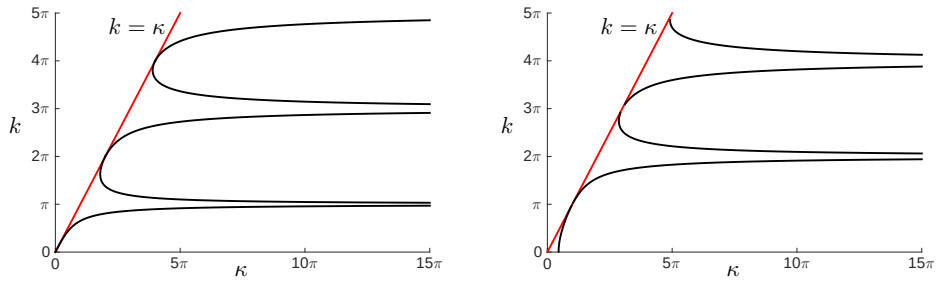

FIG. 4. *Root of* $c_+(k,\kappa) = 0$*:* $\kappa = \phi^+(k) = k\sqrt{1+\eta^2\tan^2(k/2)}$ *(left), and root of* $c_-(k,\kappa) = 0$*:* $\kappa = \phi^-(k) = k\sqrt{1+\eta^2\cot^2(k/2)}$ *(right).*

(i) $0 \le k^{\pm}_{0,0}(\kappa) < k^{\pm}_{1,0}(\kappa) < \cdots < k^{\pm}_{M^{\pm},0}(\kappa) \le |\kappa|$,

(ii) *for each* m, $k^{\pm}_{m,0}(\kappa)$ *is a continuous and monotonic function of* κ,

(iii) *as* $|\kappa| \to \infty$, $k^{+}_{m,0}(\kappa) \to m\pi$ *and* $k^{-}_{m,0}(\kappa) \to (m+1)\pi$ *if* m *is odd, and* $k^{+}_{m,0}(\kappa) \to (m+1)\pi$ *and* $k^{-}_{m,0}(\kappa) \to (m+2)\pi$ *if* m *is even.*

Proof. Solving $c_+(k,\kappa) = 0$ yields

$$\kappa = \pm\,\phi_+(k) := \pm\, k\sqrt{1+\eta^2\tan^2(k/2)}, \quad k \ge 0.$$

Without loss of generality, we consider $\kappa \ge 0$ and $\kappa = \phi_+(k)$.

Decompose the domain of the definition for $\phi_+(k)$ as nonoverlapping intervals:

$$D(\phi_+) = \bigcup_{m=0}^{\infty} \Big(\big[2m\pi, (2m+1)\pi\big) \bigcup \big((2m+1)\pi, (2m+2)\pi\big) \Big).$$

Then for $k \in \big[2m\pi, (2m+1)\pi\big)$, $\phi_+(k)$ is monotonic increasing and its range is $\big[2m\pi, +\infty\big)$ (cf. Figure 4). Therefore, the inverse

$$(\phi_+)^{-1}: \quad \big[2m\pi, +\infty\big) \to \big[2m\pi, (2m+1)\pi\big)$$

exists, which we denote by $k^{+}_{2m,0}(\kappa)$. It is clear that $k^{+}_{2m,0}(\kappa)$ is continuous and monotonic. Furthermore, $k^{+}_{2m,0}(\kappa) \in \big[2m\pi, (2m+1)\pi\big)$ and $k^{+}_{2m,0}(\kappa) \le \kappa$. As $\kappa \to \infty$, it follows that $k^{+}_{2m,0}(\kappa) \to (2m+1)\pi$.

Similarly, $\phi_+(k)$ is monotonic decreasing in the interval $((2m+1)\pi, (2m+2)\pi)$ with range $((2m+2)\pi, +\infty)$ (cf. Figure 4). The inverse $(\phi_+)^{-1}$ also exists and is denoted by $k^{+}_{2m+1,0}(\kappa)$. We have $k^{+}_{2m+1,0}(\kappa) \in ((2m+1)\pi, (2m+2)\pi)$ and $|k^{+}_{2m+1,0}(\kappa)| < \kappa$. The continuity, monotonicity, and asymptotic behavior of the function are straightforward to derive.

Since the range of $k^{+}_{2m,0}(\kappa)$ and $k^{+}_{2m+1,0}(\kappa)$ does not overlap for different values of m, we may arrange the roots such that $0 \le k^{+}_{0,0} < k^{+}_{1,0} < \cdots < k^{+}_{M,0} \le \kappa$. Similarly, by solving $c_-(k,\kappa) = 0$ we obtain

$$\kappa = \pm\,\phi_-(k) := \pm\, k\sqrt{1+\eta^2\cot^2(k/2)}, \quad k \ge 0.$$

An analogous argument as above leads to the assertion for the roots of $c_-(k,\kappa)$. ∎

Next we derive the asymptotic expansion of the roots for p and q. Note that $kd \ll 1$ in the homogenization regime (H1); we may restrict the discussion in the bounded domain $D_M := \{z : |z| \le M\}$ on the complex k-plane, where $M > 0$ is a fixed constant. In addition, for a given κ, p and q are analytic with respect to k in D_M except for the cut-off frequency $k = \kappa$; thus we consider k which is away from this cut-off frequency. To this end, let us define the domain

$$D_{\kappa,\delta,M} := \{z : |z| \le M\} \backslash B_\delta(\kappa),$$

where δ is a positive constant and $B_\delta(z)$ is the disk with radius δ centered at z on the complex plane. Let $k^\pm_{m,0}$ be the roots of $c_\pm(k,\kappa) = 0$ as given in Lemma 3.1. Note that $\partial_k c_\pm(k^\pm_{m,0},\kappa) = 0$ only if $\kappa = 0$ or $\partial_k \phi^\pm(k_{m,0}) = 0$. They hold on a countable set on the (κ,k)-plane, as observed from the definition of $\phi^\pm(k)$ and Figure 4. If $k_{m,0} \in D_{\kappa,\delta,M}$, we obtain the following asymptotic expansion in the neighborhood of $k^\pm_{m,0}$.

THEOREM 3.2. *For each κ, if $k_{m,0} \in D_{\kappa,\delta,M}$ and $\partial_k c_\pm(k^\pm_{m,0},\kappa) \neq 0$, then in the neighborhood $B_{\delta/2}(k^\pm_m)$, the roots of $p(k;\kappa,d,\varepsilon) = 0$ and $q(k;\kappa,d,\varepsilon) = 0$ have the following asymptotic expansion:*

$$k^\pm_m = k^\pm_m(\kappa,\varepsilon) = k^\pm_{m,0}(\kappa) + \frac{1}{\partial_k c_\pm(k^\pm_{m,0},\kappa)}\left(\frac{1}{\alpha(k^\pm_{m,0},\kappa)} + \frac{3\ln 2}{\pi}\right)\varepsilon + O(\varepsilon^2). \tag{3.3}$$

Note that

$$p = c_+(k,\kappa)\alpha(k,\kappa) + \frac{3\ln 2\cdot\alpha}{\pi}\varepsilon + \varepsilon + O(s(\varepsilon)),$$
$$q = c_-(k,\kappa)\alpha(k,\kappa) + \frac{3\ln 2\cdot\alpha}{\pi}\varepsilon + \varepsilon + O(t(\varepsilon)),$$

and $k^\pm_{m,0}$ are roots of the leading-order terms $c_\pm(k,\kappa) = 0$. Hence the proof of the theorem follows the same perturbation argument as the one for Lemma 4.2 in [24], and we do not repeat it here.

Remark 3.1. For a given κ, from Lemma 3.1, we have $|k^\pm_{m,0}(\kappa)| < |\kappa|$. By assuming that $k_{m,0}$ is away from the cut-off frequency such that $k_{m,0} \in D_{\kappa,\delta,M}$, $|k^\pm_m(\kappa)| < |\kappa|$ holds true for $k^\pm_m$ obtained above.

Remark 3.2. Since both $\partial_k c_\pm(k^\pm_{m,0},\kappa)$ and $\alpha(k^\pm_{m,0},\kappa)$ are real numbers, $k^\pm_{m,0}$ and the $O(\varepsilon)$ term in the above asymptotic expansion are real. In fact, since $|k^\pm_m| < |\kappa|$, it can be argued by the variational method that $k^\pm_m$ are real eigenvalues. We refer to section 4.2 of [24] for a complete discussion. Therefore, the $O(\varepsilon^2)$ term in the asymptotic expansion is real too.

3.2. Asymptotic expansion of eigenmodes and surface bound states. For a given κ, recall that the eigenvectors for the corresponding two eigenvalues of $\mathbb{M} + \mathbb{I}$ are $[1 \quad 1]^T$ and $[1 \quad -1]^T$. Therefore, if k is an eigenvalue of the scattering operator such that $\lambda_1 = 0$ or $\lambda_2 = 0$, the solution to the homogeneous linear system

$$(\mathbb{M} + \mathbb{I})\begin{bmatrix} \langle \boldsymbol{\varphi}, \mathbf{e}_1\rangle \\ \langle \boldsymbol{\varphi}, \mathbf{e}_2\rangle \end{bmatrix} = 0$$

is given by

$$\begin{bmatrix} \langle \boldsymbol{\varphi}, \mathbf{e}_1\rangle \\ \langle \boldsymbol{\varphi}, \mathbf{e}_2\rangle \end{bmatrix} = c_1\begin{bmatrix} 1 \\ 1 \end{bmatrix} \quad \text{and} \quad \begin{bmatrix} \langle \boldsymbol{\varphi}, \mathbf{e}_1\rangle \\ \langle \boldsymbol{\varphi}, \mathbf{e}_2\rangle \end{bmatrix} = c_2\begin{bmatrix} 1 \\ -1 \end{bmatrix},$$

respectively, for some constant c_1 and c_2.

We derive the eigenmode of the homogeneous scattering problem. Without loss of generality, let us set $c_1 = c_2 = 1$. First consider the far-field zones $\Omega_1^+ := \{x \mid x_2 > 2\}$ and $\Omega_1^- := \{x \mid x_2 < -1\}$ above and below the slab, respectively. By the quasi periodicity of the solution, we may restrict the discussion to the domain $\Omega_1^+ \cap \Omega^{(0)}$. Observe that the scattered field

(3.4)
$$u_\varepsilon^s(x) = \int_{\Gamma_\varepsilon^+} g^e(x,y)\frac{\partial u_\varepsilon(y)}{\partial \nu}ds_y = -\varepsilon \int_0^1 g^e(x,(\varepsilon Y,1))\varphi_1(Y)dY, \quad x \in \Omega_1^+ \cap \Omega^{(0)}.$$

Let $k = k_m^+$, then $\langle \boldsymbol{\varphi}, \mathbf{e}_1 \rangle = 1$. In addition,

$$g^e(x,(\varepsilon Y,1)) = g^e(x,(0,1))\,(1+O(\varepsilon)) \quad \text{for } x \in \Omega_1^+ \cap \Omega^{(0)}, \tag{3.5}$$

and we obtain

$$u_\varepsilon^s(x) = -\varepsilon\,(1+O(\varepsilon))\,g^e(x,(0,1)) \quad \text{for } x \in \Omega_1^+ \cap \Omega^{(0)}. \tag{3.6}$$

Note that $\kappa_n \sim O(1/\varepsilon)$ and $\zeta_n(k) = \sqrt{k^2-\kappa_n^2} \sim O(1/\varepsilon)$ for $n \neq 0$, since $d \sim \varepsilon$. Therefore,

$$\begin{aligned} g^e(x,(0,1)) = 2g^d(x,(0,1)) &= -\frac{i}{d}\sum_{n=-\infty}^{\infty}\frac{1}{\zeta_n(k_m^+)}e^{i\kappa_n(x_1)+i\zeta_n(k_m^+)|x_2-1|} \\ &= -\frac{i}{d}\frac{1}{\zeta_0(k_m^+)}e^{i\kappa x_1+i\zeta_0(k)|x_2-1|} + O(e^{-2\pi\eta/\varepsilon\cdot|x_2-1|}). \end{aligned} \tag{3.7}$$

Substituting into (3.6) and using the fact that $|\kappa| > k_m^+$ yields that

$$u_\varepsilon^s(x) = \frac{\eta}{\sqrt{\kappa^2-(k_m^+)^2}}e^{i\kappa x_1-\sqrt{\kappa^2-(k_m^+)^2}\,|x_2-1|} + O(\varepsilon) \quad \text{for } x \in \Omega_1^+ \cap \Omega^{(0)}. \tag{3.8}$$

Similarly, by using $\langle \boldsymbol{\varphi}, \mathbf{e}_2 \rangle = 1$, we have

$$u_\varepsilon^s(x) = \frac{\eta}{\sqrt{\kappa^2-(k_m^+)^2}}e^{i\kappa x_1-\sqrt{\kappa^2-(k_m^+)^2}\,|x_2|} + O(\varepsilon) \quad \text{for } x \in \Omega_1^- \cap \Omega^{(0)}. \tag{3.9}$$

Namely, the eigenmode is a surface bound-state mode that decays exponentially above and below the slab. The same holds for the eigenmode corresponding to $k = k_m^-$.

In the reference slit $S_\varepsilon^{(0)}$, by noting that

$$\begin{cases} \Delta u_\varepsilon + k^2 u_\varepsilon = 0 \quad \text{in } S_\varepsilon^{(0)}, \\ \dfrac{\partial u_\varepsilon}{\partial x_1} = 0 \quad \text{on } x_1 = 0,\ x_1 = \varepsilon, \end{cases}$$

we may expand u_ε as the sum of wave-guide modes as follows:

$$u_\varepsilon(x) = a_0 e^{ikx_2} + b_0 e^{ik(1-x_2)} + \sum_{m\geq 1}\left(a_m e^{-k_2^{(m)}x_2} + b_m e^{-k_2^{(m)}(1-x_2)}\right)\cos\frac{m\pi x_1}{\varepsilon}, \tag{3.10}$$

where $k_2^{(m)} = \sqrt{(m\pi/\varepsilon)^2 - k^2}$. Taking the derivative of (3.10) and evaluating on the slit apertures, it follows that

$$\frac{\partial u_\varepsilon}{\partial x_2}(x_1, 1) = ika_0 e^{ik} - ikb_0 + \sum_{m\geq 1} \left(-a_m e^{-k_2^{(m)}} + b_m\right) k_2^{(m)} \cos\frac{m\pi x_1}{\varepsilon}, \tag{3.11}$$

$$\frac{\partial u_\varepsilon}{\partial x_2}(x_1, 0) = ika_0 - ikb_0 e^{ik} + \sum_{m\geq 1} \left(-a_m + b_m e^{-k_2^{(m)}}\right) k_2^{(m)} \cos\frac{m\pi x_1}{\varepsilon}. \tag{3.12}$$

For $k = k_m^+$, recall that

$$\langle \boldsymbol{\varphi}, \mathbf{e}_1\rangle = \langle \boldsymbol{\varphi}, \mathbf{e}_2\rangle = 1,$$

and from (2.26),

$$\boldsymbol{\varphi} = -(\beta + \tilde{\beta})(\mathbb{L}^{-1}\mathbf{e}_1 + \mathbb{L}^{-1}\mathbf{e}_2).$$

Therefore, it can be shown that

$$a_0 = a_0^+ = \frac{e^{-ik}}{(1 - e^{ik})}, \quad b_0 = b_0^+ = \frac{e^{-ik}}{(1 - e^{ik})},$$

and

$$|a_m| \leq C/\sqrt{m}, \quad |b_m| \leq C/\sqrt{m} \quad \text{for } m \geq 1.$$

A similar calculation for $k = k_m^+$ leads to

$$a_0 = a_0^- = -\frac{e^{-ik}}{(1 + e^{ik})}, \quad b_0 = b_0^- = -\frac{e^{ik}}{(1 + e^{ik})}.$$

Therefore, for a given κ, the eigenmode in the slit region $S_\varepsilon^{(0),int} := \{x \in S_\varepsilon^{(0)} \mid x_2 \gg \varepsilon, 1 - x_2 \gg \varepsilon\}$ adopts the following asymptotical expansion:

$$u_\varepsilon(x) = a_0^\pm e^{ikx_2} + b_0^\pm e^{ik(1-x_2)} + O\left(e^{-1/\varepsilon}\right)$$

for the eigenvalue $k = k_m^\pm$.

3.3. Homogenization and effective medium theory. As $\varepsilon \to 0$, by the homogenization theory, one expects that the scattering by the slab with an array of slits is equivalent to the scattering by a homogeneous effective slab. To this end, let us consider an incident wave $u^i = e^{i(\kappa x_1 - \zeta(x_2-1))}$, where $\kappa = k\sin\theta$ and $\zeta = k\cos\theta$, that impinges on the slab. We calculate the total field u_ε in the far-field zone. This procedure is parallel to the one presented in section 3.2. First, it is clear that the scattered field u_ε^s is given by (3.4) in $\Omega_1^+ \cap \Omega^{(0)}$. Using the asymptotic expansion of the Green function (3.5), it follows that

$$u_\varepsilon^s(x) = -\varepsilon\,(1 + O(\varepsilon)) \cdot g^e(x, (0,1)) \cdot \int_0^1 \varphi_1(Y)dY \quad \text{for } x \in \Omega_1^+ \cap \Omega^{(0)}.$$

An application of the asymptotic expansions for the Green function in (3.7) and $\langle \boldsymbol{\varphi}, \mathbf{e}_1\rangle$ in Lemma 2.11 leads to

$$\begin{aligned} u_\varepsilon^s(x) &= -\varepsilon\,(1 + O(\varepsilon)) \cdot \left(-\frac{i}{d}\frac{1}{\zeta_0(k)} e^{i\kappa x_1 + i\zeta_0(k)|x_2 - 1|} + O(e^{-1/\varepsilon})\right) \\ &\quad \cdot (\alpha + O(r(\varepsilon))) \left(\frac{1}{p} + \frac{1}{q}\right) \\ &= \frac{i\varepsilon\alpha}{d\,\zeta} \cdot \left(\frac{1}{p} + \frac{1}{q}\right) \cdot e^{i(\kappa x_1 + \zeta(x_2-1))} \cdot (1 + O(\varepsilon))\,. \end{aligned} \tag{3.13}$$

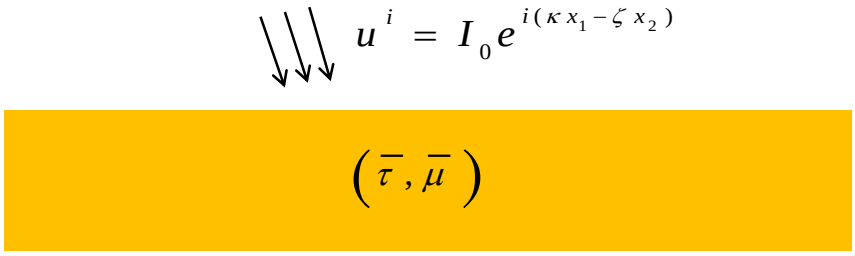

FIG. 5. *The effective layered medium as* $\varepsilon \to 0$.

Therefore, by virtue of Lemma 2.1 and the relation $\varepsilon = \eta d$,

$$u_\varepsilon(x) = u^i(x) + \left[1 + \frac{i\eta\alpha}{\zeta} \cdot \left(\frac{1}{p} + \frac{1}{q}\right) \cdot (1 + O(\varepsilon))\right] \cdot e^{i(\kappa x_1 + \zeta(x_2 - 1))} \quad \text{for } x \in \Omega_1^+ \cap \Omega^{(0)}.$$

A straightforward calculation based on (3.1) and (3.2) gives

$$\alpha \cdot \left(\frac{1}{p} + \frac{1}{q}\right) = \frac{2\zeta^2 k - i \cdot 2\zeta\eta \cdot k^2 \tan k}{-(\zeta^2 + \eta^2 k^2)\tan k - i \cdot 2\zeta\eta k} (1 + O(\varepsilon)).$$

We substitute the above into (3.13) and obtain

$$u_\varepsilon(x) = u^i(x) + R \cdot e^{i(\kappa x_1 + \zeta(x_2 - 1))} \quad \text{for } x \in \Omega_1^+ \cap \Omega^{(0)}, \tag{3.14}$$

where the reflection coefficient

$$R = \frac{i \cdot (-\zeta^2 + \eta^2 k^2)\tan k}{-i \cdot (\zeta^2 + \eta^2 k^2)\tan k + 2\zeta\eta k} \cdot (1 + O(\varepsilon)). \tag{3.15}$$

Similarly, it can be obtained that the transmitted field below the slab is

$$u_\varepsilon(x) = T \cdot e^{i(\kappa x_1 - \zeta x_2)} \quad \text{for } x \in \Omega_1^- \cap \Omega^{(0)}, \tag{3.16}$$

where the transmission coefficient

$$T = \frac{2\zeta\eta k}{-i \cdot (\zeta^2 + \eta^2 k^2)\sin k + 2\zeta\eta k \cos k} \cdot (1 + O(\varepsilon)). \tag{3.17}$$

Now let us derive the effective slab as $\varepsilon \to 0$. Denote the relative permittivity and the permeability of the effective medium in the slab by $\bar{\tau}$ and $\bar{\mu}$, respectively, and consider the layered medium as depicted in Figure 5. The corresponding scattering problem is formulated as

$$\nabla \cdot \left(\frac{1}{\tau}\nabla u\right) + k^2 \mu u = 0, \tag{3.18}$$

where

$$\tau(x_1, x_2) = \begin{cases} 1, & x_2 > 1 \text{ or } x_2 < 0, \\ \bar{\tau}, & 0 < x_2 < 1. \end{cases} \quad \text{and} \quad \mu(x_1, x_2) = \begin{cases} 1, & x_2 > 1 \text{ or } x_2 < 0, \\ \bar{\mu}, & 0 < x_2 < 1. \end{cases}$$

We look for $\bar{\tau}$ and $\bar{\mu}$ such that the associated far-field u recovers the leading-order term of the far-field u_ε given by (3.14)–(3.17).

THEOREM 3.3. *Let*

$$\bar{\tau} = \begin{bmatrix} \infty & 0 \\ 0 & 1/\eta \end{bmatrix} \quad \textit{and} \quad \bar{\mu} = \eta,$$

and let $u^i = I_0 e^{i(\kappa x_1 - \zeta(x_2-1))}$, *where* $\kappa = k\sin\theta$ *and* $\zeta = k\cos\theta$, *be the incident wave. Then the total field for the scattering problem* (3.18) *has the following form:*

$$u(x_1,x_2) = \begin{cases} I_0 e^{i(\kappa x_1 - \zeta(x_2-1)} + R_0 e^{i(\kappa x_1 + \zeta(x_2-1))}, & x_2 > 1, \\ T_0 e^{i(\kappa x_1 - \zeta x_2)}, & x_2 < 0. \end{cases}$$

The reflection and transmission coefficients are given by

$$R_0 = \frac{i\cdot(-\zeta^2+\eta^2k^2)\tan k}{-i\cdot(\zeta^2+\eta^2k^2)\tan k + 2\zeta\eta k}\cdot I_0, \quad T_0 = \frac{2\zeta\eta k}{-i\cdot(\zeta^2+\eta^2k^2)\sin k + 2\zeta\eta k\cos k}\cdot I_0.$$

Proof. If $\bar{\tau}$ and $\bar{\mu}$ are given as in the theorem, then the solution to the scattering problem can be written as follows in each layer:

$$u(x_1,x_2) = \begin{cases} I_0 e^{i(\kappa x_1 - \zeta(x_2-1))} + R_0 e^{i(\kappa x_1 + \zeta(x_2-1))}, & x_2 > 1, \\ a^+ e^{i(\kappa x_1 + k x_2)} + a^- e^{i(\kappa x_1 - k x_2)}, & 0 < x_2 < 1, \\ T_0 e^{i(\kappa x_1 - \zeta x_2)}, & x_2 < 0. \end{cases}$$

By imposing the continuity conditions along the interfaces $x_2 = 0$ and $x_2 = 1$,

$$\begin{aligned} u(x_1,0-) = u(x_1,0+), \quad \partial_{x_2}u(x_1,0-) = \eta\partial_{x_2}u(x_1,0+); \\ u(x_1,1-) = u(x_1,1+), \quad \partial_{x_2}u(x_1,1-) = \eta\partial_{x_2}u(x_1,1+), \end{aligned}$$

we obtain the following linear system for (R_0, T_0, a^+, a^-):

$$\begin{aligned} a^+ + a^- = T_0, \qquad & -i\zeta T_0 = i\eta k(a^+ - a^-), \\ e^{ik}a^+ + c^{-ik}a^- = I_0 + R_0, \quad & i\eta k(e^{ik}a^+ - e^{-ik}a^-) = i\zeta(-I_0 + R_0). \end{aligned}$$

This can be further reduced to the following system:

$$\left[-i\tan k\cdot(1+\tilde{\zeta}^2) + 2\tilde{\zeta}\right] R_0 = I_0\cdot i\cdot(1-\tilde{\zeta}^2)\tan k, \tag{3.19}$$

$$\left[-i\tan k\cdot(1+\tilde{\zeta}^2) + 2\tilde{\zeta}\right] T_0 = I_0\cdot 2\tilde{\zeta}/\cos k, \tag{3.20}$$

$$\frac{1}{2}\left(1-\tilde{\zeta}\right) T_0 - a^+ = 0, \tag{3.21}$$

$$\frac{1}{2}\left(1+\tilde{\zeta}\right) T_0 - a^- = 0, \tag{3.22}$$

where $\tilde{\zeta} = \zeta/(\eta k)$. Solving (3.19) and (3.20) proves the assertion. ∎

Next, we demonstrate the dispersion relation for the homogenized layered medium and recover the leading-order term of the dispersion relation $k_m^{\pm}(\kappa)$ given in Theorem 3.2.

THEOREM 3.4. *If*

$$\bar{\tau} = \begin{bmatrix} \infty & 0 \\ 0 & 1/\eta \end{bmatrix} \quad \textit{and} \quad \bar{\mu} = \eta,$$

then the dispersion relation for the layered medium has two branches given by

$$\kappa = k\sqrt{1+\eta^2\tan^2(k/2)} \quad \textit{and} \quad \kappa = k\sqrt{1+\eta^2\cot^2(k/2)}. \tag{3.23}$$

Moreover, the corresponding eigenmode for each branch has the following form:

$$u(x_1,x_2) = \begin{cases} R_0 e^{i\kappa x_1+\sqrt{\kappa^2-k^2}x_2}, & x_2>1, \\ a^+e^{i(\kappa x_1+kx_2)} + a^-e^{i(\kappa x_1-kx_2)}, & 0<x_2<1, \\ e^{i\kappa x_1-\sqrt{\kappa^2-k^2}x_2}, & x_2<0, \end{cases}$$

where

$$R_0 = \frac{i\sin k}{2}\cdot\left(\frac{\eta k}{\zeta}-\frac{\zeta}{\eta k}\right), a^+ = \frac{1}{2}\left(1-\frac{\zeta}{\eta k}\right), a^- = \frac{1}{2}\left(1+\frac{\zeta}{\eta k}\right).$$

Proof. To obtain the dispersion relation, we solve for (k,κ) such that there exists nontrivial solutions to the linear system (3.19)–(3.22) when $I_0 = 0$. This implies that

$$-i\tan k\cdot(1+\tilde{\zeta}^2)+2\tilde{\zeta}=0.$$

Solving the above equation yields

$$\tilde{\zeta} = \frac{\zeta}{\eta k} = i\tan(k/2) \quad \text{or} \quad \tilde{\zeta} = \frac{\zeta}{\eta k} = -i\cot(k/2).$$

Using the relation $\kappa^2+\zeta^2=k^2$, it follows that

$$\kappa^2 = k^2(1+\eta^2\tan^2(k/2)) \quad \text{or} \quad \kappa^2 = k^2(1+\eta^2\cot^2(k/2)).$$

Finally, the corresponding nontrivial solutions to the above linear system are

$$T_0 = C, \quad R_0 = \frac{ie^{-i\zeta}}{2}\sin k\cdot\left(\frac{\eta k}{\zeta}-\frac{\zeta}{\eta k}\right)C,$$
$$a^+ = \frac{1}{2}\left(1-\frac{\zeta}{\eta k}\right)C, \quad a^- = \frac{1}{2}\left(1+\frac{\zeta}{\eta k}\right)C$$

for some constant C. By taking $C=1$, we proved the second part of the theorem. ∎

3.4. Surface plasmon for plasmonic metals and perfect conductors with slits. It is known that surface plasmon modes can be supported on the flat interface between dielectric and noble metals. Let the permittivity of the dielectric and the metal be τ_1 and τ_2, respectively. For metals, we assume that $\operatorname{Re}\tau_2<0$. Such metals are also called plasmonic metals. Then it can be calculated that, for a metallic slab with thickness ℓ as shown in Figure 6 (left), the following bound states (localized surface plasmonic modes) exist along the interfaces of the dielectric-metal medium (cf. [26])

$$u(x_1,x_2) = \begin{cases} e^{i\kappa x_1-\sqrt{\kappa^2-k^2\tau_1}\,x_2}, & x_2>0, \\ a^+e^{i(\kappa x_1+\sqrt{\kappa^2-k^2\tau_2}\,x_2)} + a^-e^{i(\kappa x_1-\sqrt{\kappa^2-k^2\tau_2}\,x_2)}, & 0<x_2<\ell, \\ t_0 e^{i\kappa x_1+\sqrt{\kappa^2-k^2}x_2}, & x_2<0. \end{cases} \tag{3.24}$$

In addition, the dispersion relations are given by

$$\tanh(\sqrt{\kappa^2-k^2\tau_2}\ell)+\frac{\tau_1\sqrt{\kappa^2-k^2\tau_2}}{\tau_2\sqrt{\kappa^2-k^2\tau_1}}=0 \quad \text{and} \quad \tanh(\sqrt{\kappa^2-k^2\tau_2}\ell)+\frac{\tau_2\sqrt{\kappa^2-k^2\tau_1}}{\tau_1\sqrt{\kappa^2-k^2\tau_2}}=0.$$

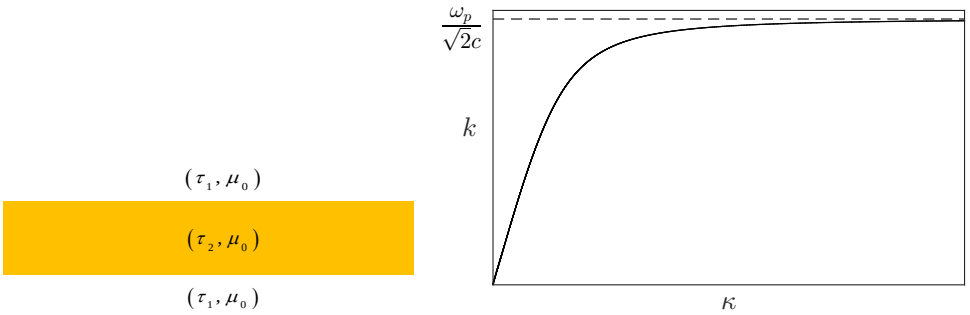

FIG. 6. *The diaelectric-metal-diaelectric medium (left) and the associated dispersion curve (right).*

For simplicity, assume that the exterior medium is vacuum so that $\tau_1 = 1$. If one applies the Drude model without damping for the metal permittivity by letting $\tau_2 = 1 - \frac{\omega_p^2}{\omega^2}$, where ω_p is the plasma frequency and it takes the value $\omega_p = 1.37 \times 10^{16}$Hz for gold [27], then the first dispersion relation is shown in Figure 6 (right), and the second dispersion relation has a similar shape.

Such localized plasmonic waves, however, do not exist for a perfect conducting slab [26]. Now if the perfect conducting slab is patterned with an array of slits as we consider here, a direct comparison of Figures 4 and 6 shows the resemblance of the dispersion curves for the plasmonic metal and the perfect conductor. Both dispersion curves lie below the light line such that $k(\kappa) < |\kappa|$ and approach certain frequencies as $\kappa \to \infty$. In addition, from (3.8), (3.9), and (3.24), the corresponding eigenmodes are both localized bound states along the slab interfaces. That is, a surface plasmonic effect mimicking that of plasmonic metals exists in a perfect conducting slab with engineered surfaces. In particular, for a perfect conducting slab with thickness ℓ, by a scaling argument, it is seen that the wavenumber $k \to \pi/\ell$ and $2\pi/\ell$, respectively, for the first branch of two dispersion curves as the κ increases to infinity, while for the plasmonic metal, the wavenumber $k \to \omega_p/(\sqrt{2}c)$ as κ increases to infinity. Therefore, $1/\ell$ determines the plasmonic frequency for the perfect conductor. As such one can tune the associated plasmonic mode in different frequencies by adjusting the thickness ℓ of the metallic slab.

3.5. Total transmission for the scattering by an incident plane wave. As discussed in previous sections, surface bound states occur when $k^{\pm}(\kappa) < |\kappa|$. Now if one considers scattering by an incident plane wave $u^i = e^{i(\kappa x_1 - \zeta(x_2 - 1))}$, where $\kappa = k \sin\theta$ and $\zeta = k\cos\theta$. Then $|\kappa| < k$ holds, and the solution to the scattering problem is unique. The corresponding reflection and transmission coefficients are given by (3.15) and (3.17). As $\varepsilon \to 0$, their limit values are the ones associated with the effective medium as stated in Theorem 3.3. In this section, we investigate the field pattern above and below the metallic slab in the limiting case of $\varepsilon \to 0$. To this end, let us rewrite the reflection coefficient R_0 and the transmission coefficient T_0 in Theorem 3.3 as

$$R_0 = \frac{i \tan k \cdot (\eta^2 - \cos^2\theta)}{-i \tan k \cdot (\eta^2 + \cos^2\theta)) + 2\eta\cos\theta}, \tag{3.25}$$

$$T_0 = \frac{2\cos\theta \cdot \eta}{-i \sin k \cdot (\eta^2 + \cos^2\theta) + 2\cos\theta \cdot \eta \cos k}. \tag{3.26}$$

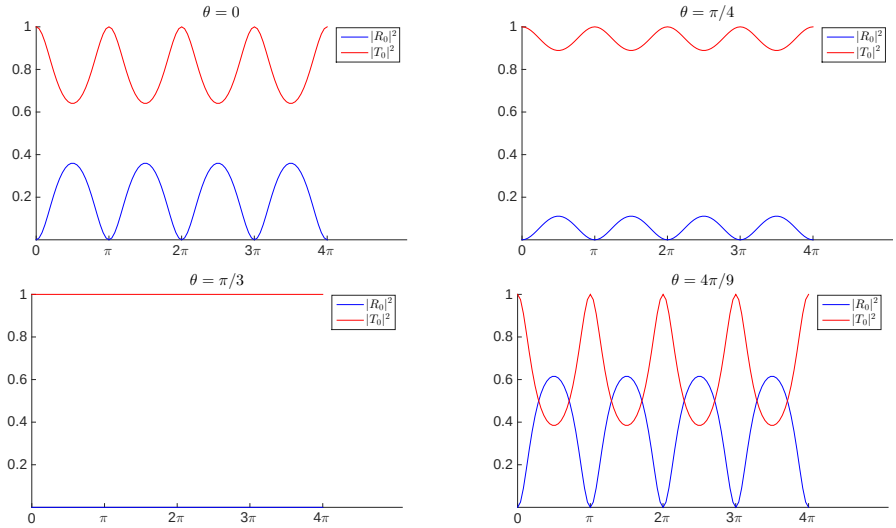

FIG. 7. $|R_0|^2$ *and* $|T_0|^2$ *for various incident angles and wavenumbers when* $\eta = 0.5$. *Note that* $|R_0|^2 + |T_0|^2 = 1$.

When $\eta = 0.5$, their amplitudes for various incident angles and wavenumbers are shown in Figure 7. It is seen that at $k = m\pi$, where m is an integer, $|T_0| = 1$ for all incident angles. That is, total transmission is achieved at $k = m\pi$ for the scattering by the homogenized slab, which is the limiting effective medium of a perfect conducting slab perorated with an array of small slits and with small periods. For the special incident angle such that $\cos\theta = \eta$, it can be calculated that $T_0 = e^{ik}$ and total transmission is obtained for all frequencies (see Figure 7). It should be pointed out that perfect transmission has also been reported for highly conductive metals patterned with narrow slits [9].

We now discuss the physical origin of the above total transmission phenomenon. Note that surface bound states associated with the slab structure do not couple an incident plane wave, since $k^{\pm}(\kappa) < |\kappa|$ holds for the real dispersion curves (3.23). On the other hand, it is evident from our analysis in section 3.1 that there exists no scattering resonance for the periodic structure in the homogenization regime (H1). Therefore, we deduce that the total transmission observed here is not due to a plasmonic resonant effect or scattering resonance. Instead, the first type of total transmission, which occurs at frequency $k = m\pi$ for some integer m, is due to the so-called Fabry–Perot resonances associated with the homogenized slab. At those frequencies, all reflected waves from the slab boundaries interfere destructively and the zero reflected wave is finally attained on top of the slab [33]. The second type of total transmission occurs for all frequencies at the special incident angle such that $\cos\theta = \eta$. This can be attributed to the so-called Brewster angle effect [2, 3].

4. Homogenization regime (H2): Nonresonant field enhancement. In the homogenization regime (H2) where $\varepsilon \ll d \ll \lambda$ (see Figure 2, bottom), we show that there exists no resonance or eigenvalue and the corresponding scattering problem (1.1)–(1.4) attains a unique solution in section 4.1. In section 4.2, we derive the asymptotic expansion of the wave fields in both the near- and far-field zones and study their enhancement in this regime. It is shown that although no enhancement is gained for the magnetic field, a strong electric field is induced in the slits and on the slit apertures. A discussion on the field enhancement for varying period d is

presented in section 4.3. Briefly speaking, the field enhancement becomes stronger as d increases. For extremely large d that still satisfies $d \ll \lambda$, the effect of periodicity is vanishing and enhancement resembles that of the single slit considered in [23] as $d \to \infty$. On the other hand, as d decreases, the field enhancement becomes weaker. In particular, if $d \sim \varepsilon$ holds, then no electromagnetic field enhancement is gained.

4.1. Nonexistence of resonance or eigenvalue. From (2.22), the homogeneous scattering problem with the incident wave $u^i = 0$ can be equivalently formulated as the operator equation

$$(\mathbb{P} + \mathbb{L})\boldsymbol{\varphi} = 0,$$

which further reduces to

$$(\mathbb{M} + \mathbb{I}) \begin{bmatrix} \langle \boldsymbol{\varphi}, \mathbf{e}_1 \rangle \\ \langle \boldsymbol{\varphi}, \mathbf{e}_2 \rangle \end{bmatrix} = 0,$$

by (2.27). Therefore, the resonances/eigenvalues of the scattering operator are roots of $\lambda_1(k;\kappa,d,\varepsilon)$ and $\lambda_2(k;\kappa,d,\varepsilon)$, the eigenvalues of $\mathbb{M}+\mathbb{I}$. Equivalently, they are roots of $p(k;\kappa,d,\varepsilon) = 0$ and $q(k;\kappa,d,\varepsilon) = 0$.

Let us define

$$\gamma(k,\kappa,d) = \frac{1}{\pi}\left(3\ln 2 + \ln\frac{\pi}{d}\right) + \left(\frac{1}{2\pi}\sum_{n\neq 0}\frac{1}{|n|} - \frac{i}{d}\sum_{n=-\infty}^{\infty}\frac{1}{\zeta_n(k)}\right), \tag{4.1}$$

where

$$\zeta_n(k) = \zeta(k,\kappa,d) = \begin{cases} \sqrt{k^2 - (\kappa + 2\pi n/d)^2}, & |\kappa + 2\pi n/d| < k, \\ i\sqrt{(\kappa + 2\pi n/d)^2 - k^2}, & |\kappa + 2\pi n/d| > k. \end{cases}$$

Then from (2.29), the definition of β in (2.18), and Lemma 2.9, we may explicitly express

$$\begin{aligned} p(k;\kappa,d,\varepsilon) &= \varepsilon + \left[\frac{\cot k}{k} + \frac{1}{k\sin k} + \varepsilon\gamma(k,\kappa,d) + \frac{1}{\pi}\varepsilon\ln\varepsilon\right]\left(\langle \mathbb{L}^{-1}\mathbf{e}_1, \mathbf{e}_1\rangle + \langle \mathbb{L}^{-1}\mathbf{e}_1, \mathbf{e}_2\rangle\right) \\ &= \varepsilon + \left[\frac{\cot k}{k} + \frac{1}{k\sin k} + \varepsilon\gamma(k,\kappa,d) + \frac{1}{\pi}\varepsilon\ln\varepsilon\right](\alpha + s(\varepsilon)), \end{aligned} \tag{4.2}$$

where $s(\varepsilon) \sim O(r(\varepsilon))$. Similarly,

$$q(k;\kappa,d,\varepsilon) = \varepsilon + \left[\frac{\cot k}{k} - \frac{1}{k\sin k} + \varepsilon\gamma(k,\kappa,d) + \frac{1}{\pi}\varepsilon\ln\varepsilon\right](\alpha + t(\varepsilon)), \tag{4.3}$$

where $t(\varepsilon) \sim O(r(\varepsilon))$. It is clear that as $k \to 0$,

$$\left(\frac{\cot k}{k} + \frac{1}{k\sin k}\right)\alpha \to \infty \quad \text{and} \quad \left(\frac{\cot k}{k} - \frac{1}{k\sin k}\right)\alpha \to -\frac{\alpha}{2}.$$

Therefore, as $\varepsilon \to 0$, $p(k;\kappa,d,\varepsilon) = 0$ and $q(k;\kappa,d,\varepsilon) = 0$ do not attain roots for $k \ll 1$. We can conclude that no resonance or eigenvalue (or singular frequency) exists for the periodic slit structure in the homogenization regime (H2).

4.2. Quantitative analysis of the electromagnetic field in the near-field and far-field zones.

4.2.1. Field enhancement in the slits. From the previous discussion, the scattering problem in the homogenization regime (H2) attains a unique solution. In this section, we investigate the electromagnetic field in both near-field and far-field zones. Note that in the reference slit $S_\varepsilon^{(0)}$ (see section 3.2), u_ε can be expanded as

$$u_\varepsilon(x) = a_0 \cos kx_2 + b_0 \cos k(1-x_2) + \sum_{m\geq 1} \left(a_m e^{-k_2^{(m)} x_2} + e^{-k_2^{(m)} x_2} \right) \cos \frac{m\pi x_1}{\varepsilon}, \tag{4.4}$$

where $k_2^{(m)} = \sqrt{(m\pi/\varepsilon)^2 - k^2}$. The following asymptotic expansion holds for u_ε in $S_\varepsilon^{(0),int} := \{x \in S_\varepsilon^{(0)} \mid x_2 \gg \varepsilon, 1-x_2 \gg \varepsilon\}$.

LEMMA 4.1. *In the slit region $S_\varepsilon^{(0),int}$, we have $u_\varepsilon(x_1,x_2) = u_0(x_2) + u_\infty(x_1,x_2)$, where*

$$u_0(x_2) = [\alpha + O(r(\varepsilon))] \left[\frac{\cos(kx_2)}{k\sin k} \left(\frac{1}{p} + \frac{1}{q} \right) + \frac{\cos(k(1-x_2))}{k\sin k} \left(\frac{1}{p} - \frac{1}{q} \right) \right], \tag{4.5}$$

and $u_\infty \sim O\left(e^{-1/\varepsilon}\right)$. Here α is defined in Lemma 2.7.

Proof. From the expansion (4.4), it follows that

$$\frac{\partial u_\varepsilon}{\partial x_2}(x_1,1) = ika_0 e^{ik} - ikb_0 + \sum_{m\geq 1} \left(-a_m e^{-k_2^{(m)}} + b_m \right) k_2^{(m)} \cos \frac{m\pi x_1}{\varepsilon}, \tag{4.6}$$

$$\frac{\partial u_\varepsilon}{\partial x_2}(x_1,0) = ika_0 - ikb_0 e^{ik} + \sum_{m\geq 1} \left(-a_m + b_m e^{-k_2^{(m)}} \right) k_2^{(m)} \cos \frac{m\pi x_1}{\varepsilon}. \tag{4.7}$$

Therefore,

$$-a_0 k\sin k = \frac{1}{\varepsilon} \int_{\Gamma_\varepsilon^+} \frac{\partial u_\varepsilon}{\partial x_2}(x_1,1)dx_1 = -\int_0^1 \varphi_1(X)dX = -[\alpha + O(r(\varepsilon))] \left(\frac{1}{p} + \frac{1}{q} \right),$$

$$b_0 k\sin k = \frac{1}{\varepsilon} \int_{\Gamma_\varepsilon^-} \frac{\partial u_\varepsilon}{\partial x_2}(x_1,0)dx_1 = \int_0^1 \varphi_2(X)dX = [\alpha + O(r(\varepsilon))] \left(\frac{1}{p} - \frac{1}{q} \right).$$

We obtain

$$a_0 = \frac{1}{k\sin k} [\alpha + O(r(\varepsilon))] \left(\frac{1}{p} + \frac{1}{q} \right), \quad b_0 = \frac{1}{k\sin k} [\alpha + O(r(\varepsilon))] \left(\frac{1}{p} - \frac{1}{q} \right). \tag{4.8}$$

For $m \geq 1$, the coefficients a_m and b_m can be obtained similarly by taking the inner product of (4.6) and (4.7) with $\cos \frac{m\pi x_1}{\varepsilon}$. Then a direct estimate leads to

$$|a_m| \leq C/\sqrt{m}, \quad |b_m| \leq C/\sqrt{m} \quad \text{for } m \geq 1, \tag{4.9}$$

where C is some positive constant independent of ε, k, and m. The proof is complete by substituting (4.8) and (4.9) into (4.4). ∎

Recall that in homogenization regime (H2), $\varepsilon \ll 1$ and $k \ll 1$. In what follows, we set $k = \varepsilon^\sigma$, where $\sigma > 0$.

LEMMA 4.2. *Let $\sigma > 0$ and $k = \varepsilon^\sigma$; then*

$$\frac{1}{p} \cdot \frac{1}{k \sin k} = \frac{1}{2\alpha}(1 + O(\varepsilon^{2\sigma}) + O(\varepsilon^{\sigma+1})) \tag{4.10}$$

and

$$\frac{1}{q} = \begin{cases} -\dfrac{2}{\alpha}\left(1 + O(\varepsilon^{2\sigma}) + O(\varepsilon^{1-\sigma})\right) & \text{if } 0 < \sigma < 1, \\ \dfrac{i \cdot d \cos\theta}{\alpha} \varepsilon^{\sigma-1}\left(1 + O(\varepsilon^{\sigma-1})\right) & \text{if } \sigma > 1. \end{cases} \tag{4.11}$$

Proof. From the expression of γ in (4.1), it is clear that

$$\gamma(k, \kappa, d) = -\frac{i}{d\, \zeta_0(k)} + O(1) = -\frac{i}{kd \cos\theta} + O(1).$$

From the explicit formulas of p and q in (4.2) and (4.3), a direct calculation yields

$$\begin{aligned} \frac{1}{p} \cdot \frac{1}{k \sin k} &= \frac{1}{(\cos k + 1)\alpha}\left(1 + O(k^2 \varepsilon \ln \varepsilon) + O(\gamma k^2 \varepsilon)\right) \\ &= \frac{1}{2\alpha(1 + O(\varepsilon^{2\sigma}))}\left(1 + O(\varepsilon^{2+2\sigma} \ln \varepsilon) + \frac{1}{d} \cdot O(\varepsilon^{1+\sigma})\right) \\ &= \frac{1}{2\alpha}\left(1 + O(\varepsilon^{2\sigma}) + \frac{1}{d} \cdot O(\varepsilon^{1+\sigma})\right). \end{aligned} \tag{4.12}$$

On the other hand,

$$\begin{aligned} q &= \left(-\frac{1}{2} + O(k^2) + \gamma\varepsilon + \frac{1}{\pi}\varepsilon \ln \varepsilon\right)\left(\alpha + t(\varepsilon)\right) + \varepsilon \\ &= -\alpha\left(\frac{1}{2} + O(\varepsilon^{2\sigma}) + \frac{i}{d \cos\theta}\varepsilon^{1-\sigma} + O(\varepsilon \ln \varepsilon)\right), \end{aligned} \tag{4.13}$$

whence the asymptotic expansion of $1/q$ follows. ∎

THEOREM 4.3. *Let $\sigma > 0$ and $k = \varepsilon^\sigma$; then $u_\varepsilon(x_1, x_2) = u_0(x_2) + u_\infty(x_1, x_2)$, where*

$$u_0(x_2) = \begin{cases} 2x_2 + O(\varepsilon^{2\sigma}) + O(\varepsilon^{1-\sigma}) & \text{if } 0 < \sigma < 1, \\ 1 + id \cdot \cos\theta\big(2x_2 - 1\big)\varepsilon^{\sigma-1} + O(\varepsilon^{\sigma+1}) + O(\varepsilon^{2(\sigma-1)}) & \text{if } \sigma > 1, \end{cases}$$

and $u_\infty \sim O\left(e^{-1/\varepsilon}\right)$.

Proof. By a combination of Lemmas 4.1 and 4.2, and the Taylor expansion, it follows that when $0 < \sigma < 1$,

$$\begin{aligned} u_0(x_2) &= (1 + O(r(\varepsilon)))\left[\frac{1}{2}\big(1 + O(\varepsilon^{2\sigma})\big)\big(\cos(kx_2) + \cos(k(1 - x_2))\big)\right. \\ &\qquad \left. -2\big(1 + O(\varepsilon^{2\sigma}) + O(\varepsilon^{1-\sigma})\big)\frac{\cos(kx_2) - \cos(k(1 - x_2))}{k \sin k}\right] \\ &= (1 + O(r(\varepsilon)))\left[1 + O(\varepsilon^{2\sigma}) - \left(1 + O(\varepsilon^{2\sigma}) + O(\varepsilon^{1-\sigma})\right)\big(1 - 2x_2\big)\right] \\ &= 2x_2 + O(\varepsilon^{2\sigma}) + O(\varepsilon^{1-\sigma}), \end{aligned}$$

while for $\sigma > 1$,

$$u_0(x_2) = (1 + O(r(\varepsilon))) \left[1 + O(\varepsilon^{\sigma+1}) + \frac{id \cdot \cos\theta}{2}\, \varepsilon^{\sigma-1} \left(1 + O(\varepsilon^{\sigma-1})\right) \left(1 - 2x_2\right)\right]$$
$$= 1 + \frac{id \cdot \cos\theta}{2}\big(1 - 2x_2\big)\varepsilon^{\sigma-1} + O(\varepsilon^{\sigma+1}) + O(\varepsilon^{2(\sigma-1)}). \qquad \square$$

From the above theorem, we see that there is no enhancement for the magnetic field u_ε in the homogenization regime (H2). However, the transition of the magnetic field u_ε along the x_2 direction resembles a linear function with a slope of 2 (for $0 < \sigma < 1$) and $O(\varepsilon^{\sigma-1})$ (for $\sigma > 1$) in the slits. This is in contrast with the incident field, which changes with a rate of $O(k)$, or $O(\varepsilon^\sigma)$, in the slits. Such fast transition of magnetic field from the upper to the lower slit aperture, compared to the incident wave, induces strong electric field enhancement as stated in the following theorem.

THEOREM 4.4. *If $\varepsilon \ll 1$ and $k = \varepsilon^\sigma$, then the electric field $E_\varepsilon = [E_{\varepsilon,1}, E_{\varepsilon,2}, 0]$ in S_ε^{int} has the following asymptotic expansion:*

$$E_{\varepsilon,1} = \begin{cases} \dfrac{2i}{\varepsilon^\sigma \sqrt{\tau_0/\mu_0}} + \min\{O(\varepsilon^\sigma), O(\varepsilon^{1-2\sigma})\} & \text{if } 0 < \sigma < 1, \\ \dfrac{d\cos\theta}{\varepsilon\sqrt{\tau_0/\mu_0}} + \min\{O(\varepsilon), O(\varepsilon^{\sigma-2})\} & \text{if } \sigma > 1, \end{cases} \qquad \text{and } E_{\varepsilon,2} \sim O(e^{-1/\varepsilon}/\varepsilon^\sigma).$$

Here τ_0 and μ_0 are the electric permittivity and magnetic permeability in the vacuum, respectively.

Proof. Note that in the TM case, the magnetic field is given by

$$H_\varepsilon = [0, 0, u_\varepsilon].$$

Therefore, by Ampere's law

$$\nabla \times H_\varepsilon = [\partial u_\varepsilon/\partial x_2, -\partial u_\varepsilon/\partial x_1, 0] = -i\omega\tau_0 E_\varepsilon.$$

For $0 < \sigma < 1$, we have

$$E_{\varepsilon,1} = \frac{2i}{k\sqrt{\tau_0/\mu_0}} + O(\varepsilon^{2\sigma}/k) + O(\varepsilon^{1-\sigma}/k) = \frac{2i}{\varepsilon^\sigma\sqrt{\tau_0/\mu_0}} + O(\varepsilon^\sigma) + O(\varepsilon^{1-2\sigma}),$$
$$E_{\varepsilon,2} = -\partial u_\infty/\partial x_1 \cdot i/\omega\tau_0 \sim O(e^{-1/\varepsilon}/k) = O(e^{-1/\varepsilon}/\varepsilon^\sigma).$$

The electric field when $\sigma > 1$ follows by a similar calcuation. $\square$

Remark 4.5. From the above theorem, we see that the enhancement for the electric field is not uniform in the low frequency regime. When $k = \varepsilon^\sigma$ with $0 < \sigma < 1$, E_ε is of order $O(1/\varepsilon^\sigma)$, or equivalently $O(1/k)$. Thus the enhancement becomes stronger as k decreases in such a scenario, while for $\sigma > 1$, E_ε is of order $O(1/\varepsilon)$, which is independent of k.

Remark 4.6. It is also observed from the previous discussion that the electric field enhancement also depends on the size of period d. Such dependence is significant when $\sigma > 1$. This will be discussed in more detail in section 4.3.

4.2.2. Field enhancement on apertures of slits. Define

$$h(X) = \frac{1}{\pi}\int_0^1 \ln|X-Y|(K^{-1}1)(Y)dY, \tag{4.14}$$

and let

(4.15)

$$\bar{\beta}^e(k,\kappa,d) := \beta^e(k,\kappa,d,\varepsilon) - \frac{1}{\pi}\ln\varepsilon = \left(\ln 2 + \ln\frac{\pi}{d}\right) + \left(\frac{1}{2\pi}\sum_{n\neq 0}\frac{1}{|n|} - \frac{i}{d}\sum_{n=-\infty}^{\infty}\frac{1}{\zeta_n(k)}\right).$$

LEMMA 4.7. *The following asymptotic for the total field holds:*

$$\begin{aligned} u_\varepsilon(x_1,1) = &-\frac{1}{\pi}\left(\frac{\alpha}{p}+\frac{\alpha}{q}\right)\cdot\varepsilon\ln\varepsilon - \left(\frac{\alpha}{p}+\frac{\alpha}{q}\right)\left(\bar{\beta}^e + h(x_1/\varepsilon)\right)\cdot\varepsilon + 2 \\ &- \left(\frac{\alpha}{p}+\frac{\alpha}{q}\right)\cdot O(\varepsilon\ln\varepsilon\cdot r(\varepsilon)) - \kappa\cdot O(\varepsilon) + O(\varepsilon\cdot r(\varepsilon)) \end{aligned} \tag{4.16}$$

and

$$\begin{aligned} u_\varepsilon(x_1,0) = &-\frac{1}{\pi}\left(\frac{\alpha}{p}-\frac{\alpha}{q}\right)\cdot\varepsilon\ln\varepsilon - \left(\frac{\alpha}{p}-\frac{\alpha}{q}\right)\left(\bar{\beta}^e + h(x_1/\varepsilon)\right)\cdot\varepsilon \\ &- \left(\frac{\alpha}{p}-\frac{\alpha}{q}\right)\cdot O(\varepsilon\ln\varepsilon\cdot r(\varepsilon)) + O(\varepsilon\cdot r(\varepsilon)) \end{aligned} \tag{4.17}$$

on the slit apertures Γ_ε^+ *and* Γ_ε^-*, respectively.*

Proof. Recall that on Γ_ε^+,

$$u_\varepsilon(x) = \int_{\Gamma_\varepsilon^+} g_\varepsilon^e(x,y)\frac{\partial u_\varepsilon(y)}{\partial\nu}ds_y + u^i + u^r.$$

Let $x_1 = \varepsilon X$, $y_1 = \varepsilon Y$. We have

$$u_\varepsilon(\varepsilon X,1) = -\int_0^1 G_\varepsilon^e(X,Y)\varepsilon\varphi_1(Y)dY + f(X).$$

Using Lemma 2.11 and the asymptotic expansion of $G_\varepsilon^e(X,Y)$ in Lemma 2.6, we obtain

$$\begin{aligned} u_\varepsilon(\varepsilon X,1) = &-\varepsilon\beta^e\left(\alpha + O(r(\varepsilon))\right)\left(\frac{1}{p}+\frac{1}{q}\right) \\ &-\frac{\varepsilon}{\pi}\left(\kappa\cdot O(1) + \frac{\alpha}{p}+\frac{\alpha}{q}\right)\int_0^1\ln|X-Y|(K^{-1}1)(Y)dY \\ &-\left(\frac{\alpha}{p}+\frac{\alpha}{q}\right)O(\varepsilon\cdot r(\varepsilon)) + O(\varepsilon\cdot r(\varepsilon)) + f(X). \end{aligned}$$

The desired expansion follows by using (4.14) and (4.15). The asymptotic expansion on the lower aperture can be obtained similarly. ∎

Now if $\sigma > 0$ and $k = \varepsilon^\sigma$, by subsituting (4.10)–(4.11) into the above lemma, it follows that

$$u(x_1,1) = 2 + O(\varepsilon\ln\varepsilon), \quad u(x_1,0) = O(\varepsilon\ln\varepsilon).$$

Therefore there is no enhancement for the magnetic field on the aperture. The enhancement of the electric field is stated in the following theorem.

THEOREM 4.8. *Let $\sigma > 0$ and $k = \varepsilon^\sigma$; then the following hold for the electric field:*

$$E_\varepsilon(x_1,1) = \begin{cases} \dfrac{2i}{\varepsilon^\sigma\sqrt{\tau_0/\mu_0}}[K^{-1}1, -h'(X), 0] + \min\{O(\varepsilon^\sigma), O(\varepsilon^{1-2\sigma})\} & \text{if } 0<\sigma<1, \\ \dfrac{d\cos\theta}{\varepsilon\sqrt{\tau_0/\mu_0}}[K^{-1}1, -h'(X), 0] + O(\varepsilon^{\sigma-2}) & \text{if } \sigma>1, \end{cases}$$

$$E_\varepsilon(x_1,0) = \begin{cases} \dfrac{2i}{\varepsilon^\sigma\sqrt{\tau_0/\mu_0}}[K^{-1}1, h'(X), 0] + \min\{O(\varepsilon^\sigma), O(\varepsilon^{1-2\sigma})\} & \text{if } 0<\sigma<1, \\ \dfrac{d\cos\theta}{\varepsilon\sqrt{\tau_0/\mu_0}}[K^{-1}1, h'(X), 0] + O(\varepsilon^{\sigma-2}) & \text{if } \sigma>1, \end{cases}$$

on the upper and lower apertures, respectively.

Proof. We derive E_ε on the upper slit apertures. The case for the lower slit apertures can be obtained similarly. Taking the derivative of (4.16) yields

$$\frac{\partial u_\varepsilon}{\partial x_1}(x_1,1) = -\left(\frac{\alpha}{p}+\frac{\alpha}{q}\right)\cdot\frac{1}{\varepsilon}h'(X)\cdot\varepsilon - \left(\frac{\alpha}{p}+\frac{\alpha}{q}\right)\cdot O(\varepsilon\ln\varepsilon\cdot r(\varepsilon)) - \kappa\cdot O(\varepsilon),$$

where $h(X)$ is defined by (4.14). Therefore, using (4.10)–(4.11), we see that

$$\frac{\partial u_\varepsilon}{\partial x_1}(x_1,1) = \begin{cases} 2h'(X) + O(\varepsilon^{2\sigma}) + O(\varepsilon^{1-\sigma}) & \text{if } 0<\sigma<1, \\ -i\cdot d\cos\theta\; h'(X)\cdot\varepsilon^{\sigma-1} + O(\varepsilon^{2(\sigma-1)}) & \text{if } \sigma>1. \end{cases} \tag{4.18}$$

On the other hand, by (2.34) it follows that

$$\frac{\partial u_\varepsilon}{\partial x_2}(x_1,1) = -K^{-1}1\cdot\left(\kappa\cdot O(\varepsilon)+\frac{\alpha}{p}+\frac{\alpha}{q}\right) + \left(\frac{\alpha}{p}+\frac{\alpha}{q}\right)\cdot O(r(\varepsilon)) + O(r(\varepsilon)).$$

An application of (4.10)–(4.11) yields

$$\frac{\partial u_\varepsilon}{\partial x_2}(x_1,1) = \begin{cases} 2K^{-1}1 + O(\varepsilon^{2\sigma}) + O(\varepsilon^{1-\sigma}) & \text{if } 0<\sigma<1, \\ -i\cdot d\cos\theta\; K^{-1}1\cdot\varepsilon^{\sigma-1} + O(\varepsilon^{2(\sigma-1)}) & \text{if } \sigma>1. \end{cases} \tag{4.19}$$

A combination of (4.18)–(4.19) and the Ampere's law leads to the desired asymptotic expansions. ∎

4.2.3. Far-field asymptotic and effective medium theory. In the far-field zone $\Omega_1^+ := \{x \mid x_2 > 2\}$ above the slits, by restricting to the reference cell $\Omega_1^+ \cap \Omega^{(0)}$, we note that the scattered field

$$u_\varepsilon^s(x) = \int_{\Gamma_\varepsilon^+} g^e(x,y)\frac{\partial u_\varepsilon(y)}{\partial\nu}ds_y.$$

An application of formula (4.19) yields

$$u_\varepsilon^s \sim O(\varepsilon) \quad \text{and} \quad u_\varepsilon^s \sim O(\varepsilon^{2\sigma-1})$$

for $0<\sigma<1$ and $\sigma>1$, respectively. The same holds true for the far-field zone below the slits. This shows that there is no electric or magnetic field enhancement in the far field. Moreover, as $\varepsilon\to 0$, the effect of the slits vanishes and the perforated perfect conducting slab becomes a homogeneous perfect conducting slab. This is very different from the case considered in the homogenization regime (H1) in section 3.3.

4.3. Electric field enhancement in the near field for varying sizes of period. From Theorems 4.4 and 4.8, it is observed that the enhancement for the electric field E_ε depends on the size of the period d. More precisely, if $k = \varepsilon^\sigma$, then for $0 < \sigma < 1$, the enhancement is of order $O(1/\varepsilon^\sigma)$ (or equivalently $O(1/k)$) and is slightly affected as d increases, since d appears in the high-order terms of E_ε, while for $\sigma > 1$, d appears in the leading-order term of E_ε. In particular, the enhancement becomes stronger as d increases. Let us set $d = O(\varepsilon^{1-\sigma-\delta})$ for some $0 < \delta < 1$. Then $d \ll \lambda$ still holds and $d \to \infty$ as $\varepsilon \to 0$ in such a scenario. By substituting d into (4.12) and (4.13), it is clear that the following holds for p and q.

LEMMA 4.9. *If $\varepsilon \ll 1$, $k = \varepsilon^\sigma$ with $\sigma > 1$, and $d = O(\varepsilon^{1-\sigma-\delta})$ with $0 < \delta < 1$, then*

$$\frac{1}{p} \cdot \frac{1}{k \sin k} = \frac{1}{2\alpha}(1 + O(\varepsilon^{2\sigma})),$$

and

$$\frac{1}{q} = -\frac{2}{\alpha}\left(1 + O(\varepsilon^{2\sigma}) + O(\varepsilon^\delta) + O(\varepsilon \ln \varepsilon)\right).$$

Following the same lines as in Theorems 4.3 and 4.4, we can obtain the asymptotic expansion for the electromagnetic field.

PROPOSITION 4.10. *If $\varepsilon \ll 1$, $k = \varepsilon^\sigma$ with $\sigma > 1$, and $d = O(\varepsilon^{1-\sigma-\delta})$ with $0 < \delta < 1$, then*

$$u = 2x_2 + O(\varepsilon^\delta) \quad \text{and} \quad E_{\varepsilon,1} = \frac{2i}{\varepsilon^\sigma \sqrt{\tau_0/\mu_0}} + O(\varepsilon^{\delta-\sigma})$$

in the slits.

Therefore, we recover the $O(1/\varepsilon^\sigma)$ order (or equivalently the $O(1/k)$ order) enhancement for $\sigma > 1$. Namely, for sufficiently large d, a uniform $O(1/k)$ enhancement for E_ε is achieved in the low frequency regime. This is consistent with the field enhancement for a single slit perorated in a perfect conducting slab (when $d = \infty$), where an enhancement order of $O(1/k)$ is obtained in the low frequency regime [23].

On the other hand, as the period d decreases, the magnitude of the electric field E_ε decreases as well. In particular, by taking the extreme case with $d = \varepsilon/\eta$ and $0 < \eta < 1$, one recovers the periodic structure in the homogenization regime (H1). A straightforward asymptotic expansion of (3.1) and (3.2) for p and q leads to the following lemma.

LEMMA 4.11. *If $\varepsilon \ll 1$, $k = \varepsilon^\sigma$, and $d = \varepsilon/\eta$ with $0 < \eta < 1$, then*

$$\frac{1}{p} \cdot \frac{1}{k \sin k} = \frac{1}{2\alpha}(1 + O(\varepsilon^\sigma))$$

and

$$\frac{1}{q} = \frac{i \cos\theta}{\eta\alpha}\varepsilon^\sigma \left(1 + O(\varepsilon^\sigma)\right).$$

A similar calculation as in Theorems 4.3 and 4.4 yields the following conclusion.

PROPOSITION 4.12. *If $\varepsilon \ll 1$, $k = \varepsilon^\sigma$, and $d = \varepsilon/\eta$ with $0 < \eta < 1$, then*

$$u = 1 + O(\varepsilon^\sigma) \quad \text{and} \quad E_{\varepsilon,1} = O(1)$$

in the slits.

Therefore, no enhancement is gained for such configuration.

5. Conclusion. In this series of two papers, we have investigated the field enhancement and anomalous diffraction for electromagnetic wave scattering by a periodic array of subwavelength slits perforated in a perfect conducting slab. The quantitative analysis of the wave field is presented in both the diffraction regime and the two homogenization regimes. It is demonstrated that the field enhancement in the diffraction regime is mainly attributed to scattering resonances. Such enhancement becomes weaker if the resonant frequency is close to the Rayleigh cut-off frequencies. In the homogenization regimes, the field enhancement can be attributed to a certain nonresonant effect. In addition, a surface plasmonic effect mimicking that of plasmonic metals exists for the periodic structure with small period, and almost total transmission can be obtained for certain incident plane waves.

Based on the studies for the single slit case in [23] and the periodic case in this series, the mechanism of the field enhancement and anomalous diffraction for subwavelength slit structures in a perfect conducting slab is now clearly understood. Along this line of research, we will explore the field enhancement and anomalous diffraction (or transmission) for a single narrow slit and an array of slits in plasmonic metallic slabs. Other than the mechanisms that are already known to occur for perfect conductors, it is expected that additional enhancement mechanisms, including surface plasmonic resonances, will be present. This will be reported in forthcoming papers.

Appendix A. Proof of Lemma 2.7 for (H1). We prove Lemma 2.7 for the homogenization regime (H1) in this section. The proof is adopted from the one in [8]. Let $\Omega_1 = (0, \frac{1}{\eta}) \times (0, \infty)$, $\Omega_2 = (0,1) \times (0, -\infty)$, and $\Omega_{1,N} = (0, \frac{1}{\eta}) \times (0, N)$, $\Omega_{2,N} = (0,1) \times (0, -N)$. We first introduce two Green functions for the domain Ω_1 and Ω_2, respectively.

For $x, y \in \Omega_1$, we define

$$\begin{aligned} G_1(x,y) &= -\sum_{n=1}^{\infty} \frac{1}{2n\pi\eta} \left(e^{-2n\pi\eta|x_2-y_2|} + e^{-2n\pi\eta|x_2+y_2|} \right) \\ &\quad \times (\cos 2n\pi\eta x_1 \cos 2n\pi\eta y_1 + \sin 2n\pi\eta x_1 \sin 2n\pi\eta y_1) \\ &= -\sum_{n=1}^{\infty} \frac{1}{2n\pi\eta} \left(e^{-2n\pi\eta|x_2-y_2|} + e^{-2n\pi\eta|x_2+y_2|} \right) \cos 2n\pi\eta(x_1 - y_1). \end{aligned}$$

It is clear that G_1 satisfies the following equations:

$$\begin{cases} \Delta_x G_1(x,y) = \delta(x-y) \quad \text{for } x \in \Omega_1, \\ \dfrac{\partial G_1(x,y)}{\partial x_2} = 0 \quad \text{for } x_2 = 0, \\ G_1(0, x_2, y) = G_1(1/\eta, x_2, y), \\ \displaystyle\int_0^{\frac{1}{\eta}} G_1(x_1, 0, y) dx_1 = 0, \\ G_1(\cdot, y) \to 0 \text{ as } x_2 \to \infty \text{ and satisfies the outgoing radiation condition (1.4).} \end{cases}$$

Moreover, when both x, y are restricted to the boundary $\{(x_1, x_2) : x_1 \in (0, \frac{1}{\eta}), x_2 = 0\}$, we have

$$G_1(x_1, 0, y_1, 0) = -\sum_{n=1}^{\infty} \frac{1}{n\pi} \cos 2n\pi\eta(x_1 - y_1) = \frac{1}{\pi} \ln |2 \sin \pi\eta(x_1 - y_1)|.$$

For $x, y \in \Omega_2$, we define

$$G_2(x,y) = -\sum_{n=1}^{\infty} \frac{1}{2n\pi} \left(e^{-2n\pi|x_2-y_2|} + e^{-2n\pi|x_2+y_2|} \right) \cos n\pi x_1 \cos n\pi y_1.$$

Then G_2 solves the following equations:

$$\begin{cases} \Delta_x G_2(x,y) = \delta(x-y), \\ \dfrac{\partial G_2(x,y)}{\partial x_2} = 0 \quad \text{for} \quad x_2 = 0, \\ \dfrac{\partial G_2(x,y)}{\partial x_1} = 0 \quad \text{for} \quad x_1 = 0 \text{ and } x_1 = 1, \\ \displaystyle\int_0^1 G_2(x_1, 0, y) dx_1 = 0, \\ G_2(\cdot, y) \to 0 \text{ as } x_2 \to -\infty \text{ and satisfies the outgoing radiation condition (1.4).} \end{cases}$$

Moreover, when both x, y are restricted to the boundary $\{(x_1, x_2) : x_1 \in (0,1), x_2 = 0\}$, we have

$$\begin{aligned} G_2(x_1, 0, y_1, 0) &= -\sum_{n=1}^{\infty} \frac{1}{n\pi} \left(\cos n\pi(x_1 - y_1) + \cos n\pi(x_1 + y_1) \right) \\ &= \frac{1}{\pi} \ln \left| 4 \sin \frac{\pi(x_1 - y_1)}{2} \sin \frac{\pi(x_1 + y_1)}{2} \right|. \end{aligned}$$

Recall that V_1 is the space of distributions in $H^{-\frac{1}{2}}(\mathbf{R})$ whose support is contained in $[0,1]$, or distributions defined in the interval $(0,1)$ whose zero extension to the whole line belongs to $H^{-\frac{1}{2}}(\mathbf{R})$. For any $\psi \in V_1$, we define two functions:

$$\begin{aligned} u_1 = K_1\psi(x_1, x_2) &= \int_0^{\frac{1}{\eta}} G_1(x_1, x_2, y_1, 0)\psi(y_1) dy_1 \\ &= \int_0^1 G_1(x_1, x_2, y_1, 0)\psi(y_1) dy_1, \end{aligned} \tag{A.1}$$

$$u_2 = K_2\psi(x_1, x_2) = \int_0^1 G_2(x_1, x_2, y_1, 0)\psi(y_1) dy_1. \tag{A.2}$$

By the Green identity, one can show that u_1 and u_2 are the unique solution to the problem

$$\begin{cases} \Delta u_1(x) = 0 \quad \text{for } x \in \Omega_1, \\ \dfrac{\partial u_1(x)}{\partial x_2} = \psi \quad \text{for } x_2 = 0, \\ u_1(0, x_2) = u_1(1/\eta, x_2), \\ \displaystyle\int_0^{\frac{1}{\eta}} u_1(x_1, 0) dx_1 = 0, \\ u_1 \to 0 \text{ as } x_2 \to \infty, \end{cases} \quad \text{and} \quad \begin{cases} \Delta u_2(x) = 0 \quad \text{for } x \in \Omega_2, \\ -\dfrac{\partial u_2(x)}{\partial x_2} = \psi \quad \text{for } x_2 = 0, \\ u_2(0, x_2) = u_2(1, x_2), \\ \displaystyle\int_0^1 u_2(x_1, 0) dx_1 = 0, \\ u_2 \to 0 \text{ as } x_2 \to -\infty, \end{cases}$$

respectively.

Let us define the following two operators associated with the trace of the functions u_1, u_2:

$$K_{1,0}\psi(x_1) = \int_0^1 G_1(x_1, 0, y_1, 0)\psi(y_1)dy_1,$$
$$K_{2,0}\psi(x_1) = \int_0^1 G_2(x_1, 0, y_1, 0)\psi(y_1)dy_1.$$

Let $K_0 = K_{1,0}+K_{2,0}$. By analyzing the singularities in the kernel of the two operators $K_{1,0}, K_{2,0}$, and using the argument in [8], it follows that $K_0 : V_1 \to (V_1)^* = V_2$ is bounded. Moreover, $K_0^* = K_0$, where K_0^* is the dual operator (see [12]) of K_0. We show as follows.

LEMMA A.1. *K_0 is invertible from V_1 to $(V_1)^*$ and its inverse is bounded.*

To establish the above result, we first prove the following identity.

LEMMA A.2. *For any $\psi \in V_1$, we have*

$$\langle K_0\psi, \psi\rangle = -\int_{\Omega_1} |\nabla u_1|^2 dx_1 dx_2 - \int_{\Omega_2} |\nabla u_2|^2 dx_1 dx_2,$$

where u_1 and u_2 are defined in (A.1) *and* (A.2) .

Proof. Note that both u_1 and u_2 are harmonic functions and can be expanded as

$$u_1 = \sum_{n>0} \left(a_{n,1} \sin 2n\pi\eta x_1 + b_{n,1} \cos 2n\pi\eta x_1\right) e^{-2n\pi\eta x_2},$$
$$u_2 = \sum_{n>0} b_{n,2} \cos n\pi x_1 e^{2n\pi x_2}$$

for some constants $a_{n,1}, b_{n,1}, b_{n,2}$.

On the other hand, from the boundary conditions

$$\frac{\partial u_1(x_1, 0)}{\partial x_2} = -\frac{\partial u_2(x_1, 0)}{\partial x_2} = \psi,$$

it follows that

$$\begin{aligned}
\int_{\Omega_1} |\nabla u_1|^2 dx_1 dx_2 &= \lim_{N\to\infty} \int_{\Omega_{1,N}} |\nabla u_1|^2 dx_1 dx_2 = \lim_{N\to\infty} \int_{\partial\Omega_{1,N}} u_1 \frac{\partial u_1}{\partial \nu} d\sigma \\
&= -\int_0^1 u_1(x_1, 0)\frac{\partial u_1(x_1, 0)}{\partial x_2} dx_1 + \lim_{N\to\infty} \int_0^{\frac{1}{\eta}} u_1(x_1, N)\frac{\partial u_1(x_1, N)}{\partial x_2} dx_1 \\
&= -\langle K_{1,0}\psi, \psi\rangle - \lim_{N\to\infty} \sum_{n=1}^{\infty} n\pi\eta e^{-4n\pi\eta N} \left(|a_{n,1}|^2 + |b_{n,1}|^2\right) \\
&= -\langle K_{1,0}\psi, \psi\rangle.
\end{aligned}$$

Similarly for u_2, we have

$$\int_{\Omega_2} |\nabla u_2|^2 dx_1 dx_2 = -\langle K_{2,0}\psi, \psi\rangle.$$

The lemma follows. ∎

Based on the above identity, we can show as follows.

LEMMA A.3. *There exists $C > 0$ such that for all $\psi \in V_1$*

$$\|K_0\psi\|_{V_2} \geq C\|\psi\|_{V_1}.$$

Proof. We consider u_2 restricted to the domain $\Omega_{2,1}$. We have

$$\int_{\Omega_{2,1}} u_2 dx_1 dx_2 = 0.$$

By Poincarés inequality, there exists a constant C_1 such that

$$\|u_2\|_{H^1(\Omega_{2,1})} \leq C_1\|\nabla u_2\|_{L^2(\Omega_{2,1})} \leq C_1\sqrt{\|K\psi\|_{V_2} \cdot \|\psi\|_{V_1}}.$$

On the other hand, note that $\psi = -\frac{\partial u_2(x_1,0)}{\partial x_2}$. By the trace theorem, we have

$$\|\psi\|_{V_1} \leq C_2\|u_2\|_{H^1(\Omega_{2,1})}$$

for some constant C_2. It follows that

$$\|\psi\|_{V_1} \leq C_1^2 C_2^2 \|K\psi\|_{V_2}.$$

This proves the lemma. ∎

Proof of Lemma A.1. From Lemma A.3, we can conclude that the map $K_0 : V_1 \to V_1^*$ is injective. This also shows that K_0^* is also injective (since $K_0^* = K_0$). As a result, $K_0(V_1)$ is dense in $(V_1)^*$. But Lemma A.3 also implies that $K_0(V_1)$ is closed in V_2. Therefore, $K_0(V_1) = (V_1)^*$ and consequently K_0 has a bounded inverse K_0^{-1} by the open mapping theorem. ∎

Proof of Lemma 2.7 *for the case* H1. For any $\psi \in V_1$, note that

$$K\psi(X) = K_0\psi - \frac{3\ln 2}{\pi}\langle\psi, 1\rangle 1 + \frac{\kappa\eta}{\sqrt{k^2-\kappa^2}}\int_0^1 (X-Y)\psi(Y)dY.$$

A direct calculation yields

$$\langle K\psi, \psi\rangle = \langle K_0\psi, \psi\rangle - \frac{3\ln 2}{\pi}|\langle\psi, 1\rangle|^2 < \langle K_0\psi, \psi\rangle.$$

Therefore, using Lemma A.3, we can show that

$$\|K\psi\|_{V_1^*} \geq C\|\psi\|_{V_1}$$

for some constant C. Similar to the proof of Lemma A.1, we can conclude that K is invertible from V_1 to V_1^* and its inverse is also bounded.

To calculate $\alpha(k,\kappa) := \langle K^{-1}1, 1\rangle$, let $\psi_0 = K^{-1}1$. Then ψ_0 depends on k and κ and we have

$$\alpha(k,\kappa) = \langle\psi_0, K\psi_0\rangle = \langle K_0\psi_0, \psi_0\rangle - \frac{3\ln 2}{\pi}|\langle\psi, 1\rangle|^2 < 0.$$

It is obvious that $\alpha(k,\kappa)$ is a real number. This completes the proof of Lemma 2.7. ∎

Acknowledgments. The authors would like to thank Professor Ping Sheng from Hong Kong University of Science and Technology, and Professor Stephen Shipman from Louisiana State University for valuable discussions. The first author gratefully acknowledges the support and hospitality provided by the IMA at the University of Minnesota during his visit and when part of this project was performed.

REFERENCES

[1] M. Abramowitz and I. Stegun, eds., *Handbook of Mathematical Functions with Formulas, Graphs, and Mathematical Tables*, NBS Appl. Math. Ser. 55, National Bureau of Standards, Washington, DC, 1964.

[2] N. Aközbek, et al., *Experimental demonstration of plasmonic Brewster angle extraordinary transmission through extreme subwavelength slit arrays in the microwave*, Phys. Rev. B, 85 (2012), 205430.

[3] A. Alù, G. D'Aguanno, N. Mattiucci, and M. J. Bloemer, *Plasmonic Brewster angle: Broadband extraordinary transmission through optical gratings*, Phys. Rev. Lett., 106 (2011), 123902.

[4] H. Ammari, M. Ruiz, W. Wu, S. Yu, and H. Zhang, *Mathematical and numerical framework for metasurfaces using thin layers of periodically distributed plasmonic nanoparticles*, Proc. R. Soc. A., 472 (2016), 20160445.

[5] H. Ammari, B. Fitzpatrick, D. Gontier, H. Lee, and H. Zhang, *A mathematical and numerical framework for bubble meta-screens*, SIAM J. Appl. Math., 77 (2017), pp. 1827–1850.

[6] G. Bao, D. Dobson, and Cox, *Mathematical studies in rigorous grating theory*, J. Opt. Soc. Amer. A, 12 (1995), pp. 1029–1042.

[7] A. Bonnet-Bendhia and F. Starling, *Guided waves by electromagnetic gratings and non-uniqueness examples for the diffraction problem*, Math. Methods Appl. Sci., 17 (1994), pp. 305–338.

[8] E. Bonnetier and F. Triki, *Asymptotic of the Green function for the diffraction by a perfectly conducting plane perturbed by a sub-wavelength rectangular cavity*, Mathods Meth. Appl. Sci., 33 (2010), pp. 772–798.

[9] G. Bouchitt and B. Schweizer, *Plasmonic waves allow perfect transmission through sub-wavelength metallic gratings*, Netw. Heterog. Media, 8 (2013), pp. 857–878.

[10] J. F. Babadjian, E. Bonnetier, and F. Triki, *Enhancement of electromagnetic fields caused by interacting subwavelength cavities*, Multiscale Model. Simul., 8 (2010), pp. 1383–1418.

[11] X. Chen, et al., *Atomic layer lithography of wafer-scale nanogap arrays for extreme confinement of electro-magnetic waves*, Nat. Commun., 4 (2013), 2361.

[12] J. B. Conway, *A Course in Functional Analysis*, 2nd ed., Springer-Verlag, New York, 1990.

[13] T. W. Ebbesen, H. J. Lezec, H. F. Ghaemi, T. Thio, and P. A. Wolff, *Extraordinary optical transmission through sub-wavelength hole arrays*, Nature, 391 (1998), pp. 667–669.

[14] F. J. Garcia-Vidal, L. Martin-Moreno, and J. B. Pendry, *Surfaces with holes in them: New plasmonic metamaterials*, J. Opt. A Pure Appl. Opt., 7 (2005), S97.

[15] F. J. Garcia-Vidal, L. Martin-Moreno, T. W. Ebbesen, and L. Kuipers, *Light passing through subwavelength apertures*, Rev. Modern Phys., 82 (2010), pp. 729–787.

[16] I. Gradshteyn and I. Ryzhik, *Table of Integrals, Series, and Products*, Academic Press, New York, 2014.

[17] C. L. Holloway, E. F. Kuester, J. A. Gordon, J. O'Hara, J. Booth, and D. R. Smith, *An Overview of the Theory and Applications of Metasurfaces: The Two-Dimensional Equivalents of Metamaterials*, IEEE Antennas Propagation Mag., 54, (2012), pp. 10–35.

[18] R. Kress, *Linear Integral Equations*, Appl. Math. Sci. 82, Springer-Verlag, Berlin, 1999.

[19] G. A. Kriegsmann, *Complete transmission through a two-dimensional diffraction grating*, SIAM J. Appl. Math., 65 (2004), pp. 24–42.

[20] L. Lewin, *Theory of Waveguides: Techniques for the Solution of Waveguide Problems*, Halsted Press, New York, 1975.

[21] J. Lin, S.-H. Oh, H.-M. Nguyen, and F. Reitich, *Field enhancement and saturation of millimeter waves inside a metallic nanogap*, Opt. Express, 22 (2014), pp. 14402–14410.

[22] J. Lin and F. Reitich, *Electromagnetic field enhancement in small gaps: A rigorous mathematical theory*, SIAM J. Appl. Math., 75 (2015), pp. 2290–2310.

[23] J. Lin and H. Zhang, *Scattering and field enhancement of a perfect conducting narrow slit*, SIAM J. Appl. Math., 77 (2017), pp. 951–976.

[24] J. Lin and H. Zhang, *Scattering by a periodic array of subwavelength slits* I*: Field enhancement in the diffraction regime*, Multiscale Model. Simul., 16 (2018), pp. 922–953.
[25] C. Linton, *The Green's function for the two-dimensional Helmholtz equation in periodic domains*, J. Engrg. Math. 33 (1998), pp. 377–401.
[26] S. Maier, *Plasmonics: Fundamentals and Applications*, Springer, New York, 2007.
[27] M. A. Ordal, et al., *Optical properties of the metals Al, Co, Cu, Au, Fe, Pb, Ni, Pd, Pt, Ag, Ti and W in the infrared and far infrared,* Appl. Opt. 22 (1983), pp. 1099–1119.
[28] J. Pendry, L. Martin-Moreno, and F. J. Garcia-Vidal, *Mimicking surface plasmons with structured surfaces*, Science, 305 (2004), pp. 847–848.
[29] S. Shipman and D. Volkov, *Guided modes in periodic slabs: Existence and nonexistence*, SIAM J. Appl. Math., 67 (2007), pp. 687–713.
[30] S. Shipman and S. Venakides, *Resonance and bound states in photonic crystal slabs*, SIAM J. Appl. Math., 64 (2003), pp. 322–342.
[31] S. Shipman, *Resonant scattering by open periodic waveguides*, in Wave Propagation in Periodic Media: Analysis, Numerical Techniques and Practical Applications, Vol. 1, M. Ehrhardt, ed., Bentham Science Publishers, Sharjah, UAE, 2010.
[32] S. A. Tretyakov, *Metasurfaces for General Transformations of Electromagnetic Fields*, Phil. Trans. R. Soc. A, 373 (2015), 20140362.
[33] M. Vaughan, *The Fabry-Perot Interferometer: History, Theory, Practice and Applications*, CRC Press, Boca Raton, Fl, 1989.